Scientific Research Publishing

# Utilization of Various Analogy of Synthetic Nanoporous Zeolites and Composite of Zeolites for Decontamination/Detoxification of CWA Simulants—An Updated Review

**Neeraj Kumar\*, Kautily Rao Tiwari, Km. Meenu, Arti Sharma, Adya Jain, Shikha Singh, Radha Tomar**

School of Studies in Chemistry, Jiwaji University, Gwalior, India
Email: *neeraj75820@gmail.com

## Abstract

In this review, we summaries the past few year work on the chemistry of CWA's and their simulants on various heterogeneous surfaces of zeolites, composites of zeolites and doped zeolite with transition metal oxides. This review elaborates an updated literature overview on the degradation of CWA's and its simulants. The data written in this review were collected from the peer-reviewed national and international literature.

## 1. Introduction

### 1.1. Zeolites

Zeolites were first of all observed in 1756 by a Swedish mineralogist, Fredish Cronstedt. Due to its high stability at extreme temperatures, these were named as "Zeolite". The word zeolite comes from two Greek words *i.e. zeo* (signifying "to boil") and *lithos* (signifying "stone") [1]. Therefore these are also known as "Boiling Stones". Zeolites are three dimensional crystalline, micro porous, hydrated aluminosilicates of alkali and alkaline earth metals. The basic structure formula of zeolite is $M_{x/n}[(AlO_2)_x(SiO_2)_y]\cdot wH_2O$, where M denotes alkali or alkaline earth metal cation; n is the valence of the cation; w is the number of water molecules per unit cell; x and y are the total number of tetrahedral per unit cell.

These are composed of primary building unit (PBU) and secondary building units (SBUs) [2] [3]. Primary building units of zeolites are the basic tetrahedral units *i.e.* $\left[SiO_4\right]^{4-}$ and $\left[AlO_4\right]^{5-}$ tetrahedrals which are linked to each other by the sharing of oxygen atoms while secondary building units are different geometrical arrangement or morphology of the tetrahedral units. The secondary building units may be simple polyhedral (cubes, hexagonal prisms) or cubo-octahedra as shown in Figure 1.

Till now, 232 unique zeolite frameworks have been identified, and over 40 naturally occurring zeolite frameworks are known [5]. Every new synthesized and naturally obtained zeolite structure has been approved by the International Zeolite Association Structure Commission (IZASC) and receives a three letter designation. Both natural and synthetic zeolites are very useful but synthetic zeolite over the natural zeolite shows higher thermal stability and purity. Hence they possess wide range of chemical properties and pore sizes [6]. According to different arrangements of these units, zeolites can be classified into eight classes: Zeolite-A, Zeolite-N-A, Zeolite-H, Zeolite-L, Zeolite-X, Zeolite-Y, Zeolite-P, Zeolite-O, Zeolite-Ω, Zeolite ZK-4 and Zeolite ZK-5 as shown in Table 1.

Nanocrystalline zeolites are nanoporous materials with crystal sizes within the range of 100 nm. They provide larger surface area with internal surface porosity [7]. Essentially, increase in the surface area provides increased adsorption of reactant molecules on its surface, which results in higher catalytic property. The various kinds of links/bonds form a variety of rings which are responsible for zeolites cages and channels of different window sizes. Zeolites consist of pores and cavities of molecular dimensions [8]. The increase in type and structural diversity of zeolites, as well as unique properties of zeolite such as thermal stability, acidity, hydrophobicity/hydrophilicity of surfaces and ion-exchange capacity, has led to variety of applications of zeolites in various industries [9]. Due to their unique ability to select molecules/atoms/ions on the basis of their respective sizes, zeolites are referred as "molecular sieves". The major properties of zeolites are: catalysis, adsorption and ion exchange. The ions and water molecules enclosed inside these cavities have considerable freedom of movement permitting ion exchange and reversible dehydration [10].

## 1.2. Framework of Zeolites

The effective size and shape of the pore opening are determined by following steps:

- Configuration of T (*i.e.* $Si^{4+}$ and $Al^{3+}$ ion) and O atoms relative to each other,
- $SiO_2/Al_2O_3$ ratio,
- Size of cation,
- Location of cation,
- Temperature.

Zeolite containing the pore openings is referred as small, medium and large on the basis of number of members in the ring. The 8-membered ring have small pore size, diameters of about 0.30 - 0.45 nm (e.g. zeolite A), 10-membered ring

has medium pore size, diameters of about 0.45 - 0.60 nm (e.g. ZSM-5), while 12-membered ring has large pore opening, diameter of about 0.6 - 0.8 nm (e.g. zeolites X, Y). 7, 9, 11, 14, 16, 18 and 20 membered ring was also discovered recently [11]. Some other examples of zeolites with their pore size and ring size are shown in Table 2. The framework of zeolite is greatly affected by building elements *i.e.* silicon (Si) and aluminium (Al). Silicon and aluminium play an effective role in defining different properties of zeolites (thermal stability, catalytic property etc.). On altering the ratio of silicon and aluminium, modification of zeolite takes place (*i.e.* from zeolite X to zeolite Y) [12]. **Breck** *et al.* [2] had reported that this modification occurs when Si/Al ratio is 1.5. When the ratio is lower than this critical point then it characterize zeolite X composition while higher than the critical point characterize zeolite Y composition [13].
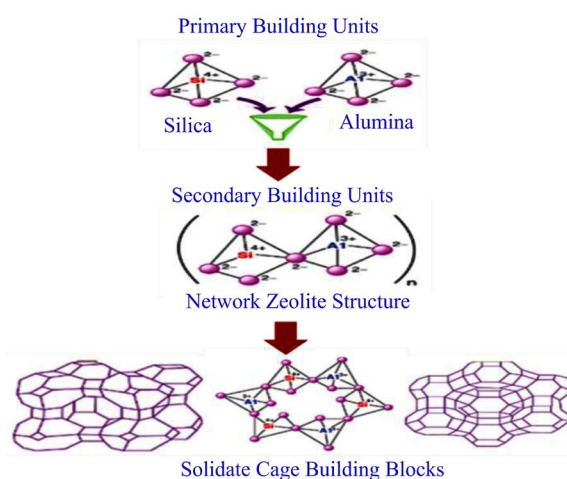


**Figure 1.** Rearrangements of PBU and SBU to form zeolite framework [4].

**Table 1.** Typical chemical formula of different zeolites [7] [14].

| Zeolites | Typical oxide formula |
|----------|----------------------|
| Zeolites A | $Na_2O. Al_2O_3. 2SiO_2. 4\text{-}5H_2O$ |
| Zeolites N-A | $(Na, TMA)_2 O. Al_2O_3. 4\text{-}8SiO_2. 7H_2O; TMA - (CH_3)4N^+$ |
| Zeolites H | $K_2O. Al_2O_3. 2SiO_2. 4H_2O$ |
| Zeolites L | $(K_2Na_2)O. Al_2O_3. 6SiO_2. 5H_2O$ |
| Zeolites X | $Na_2O. Al_2O_3. 2\text{-}5SiO_2. 6H_2O$ |
| Zeolites Y | $Na_2O.Al_2O_3. 4\text{-}8SiO_2. 8\text{-}9H_2O$ |
| Zeolites P | $Na_2O. Al_2O_3. 2\text{-}5SiO_2. 5H_2O$ |
| Zeolites O | $(Na_2, K_2, TMA_2)O. Al_2O_3. 7SiO_2. 3\text{-}5H_2O;TMA - (CH_3)4N^+$ |
| Zeolites Ω | $(Na, TMA)_2 O. Al_2O_3. 7SiO_2. 5H_2O; TMA - (CH_3)4N^+$ |
| Zeolites ZK-4 | $0.85 Na_2O. 0.15(TMA)_2 O. Al_2O_3. 3SiO_2. 6H_2O$ |
| Zeolites ZK-5 | $(R,Na_2)O. Al_2O_3. 4\text{-}6 SiO_2. 6H_2O$ |

Table 2. Zeolite pores and ring size.

| Zeolite Type | Pore size (nm) | Ring size |
| --- | --- | --- |
| MCM-22, 49 | 0.6 | 10-membered |
| UTD-1 | 1.0 | 14-membered |
| CIT-5 | 0.8 | 14-membered |
| EMC-2 | 0.7 | 12-membered |
| Colverite | 1.3 | 20-membered |

High silica content in zeolite shows catalytic properties [15] [16]. Therefore to incorporate higher catalytic property in zeolite dealumination method (chemical and structural modifications take place) is applied. EDTA has the capability to remove half of the framework aluminium atoms while treating with silicon tetrachloride, Al atoms get replaced by silicon atoms [17] [18]. Thus, greater catalytic activity can be achieved. It has been reported that at lower temperature small crystals are synthesized as compared to higher temperature. Lower than 140°C yield amorphous crystals, at 140°C smallest crystals and above 140°C large crystals were observed. Therefore crystal size is directly related to temperature change, on increasing the temperature, crystal size increases [19].

### 1.3. Properties of Zeolites

There are various properties of zeolites such as physical and chemical, ion exchange, catalytic, adsorption, minrological-morphological properties, crystal structure, framework of zeolite and surface morphology makes zeolite as an useful nanomaterial for multiple applications. The properties of zeolite are discussed below.

### 1.3.1. Physical Properties

The most important physical properties of zeolite are specific gravity (2 - 2.8 g/cm$^3$), bulk density, thermal stability, cation exchange proerty and specific surface area. The physical properties of zeolite depend on pore volume of zeolite, their void volume and dissolution of particles in solvents. The most common and general property is their particle size, large variation (2 µm - 800 nm) in particle size permit approxamitely 10% - 60% material by weight to the sieves of zeolite (adsorption) [20] [21].

### 1.3.2. Chemical Properties

Zeolite comprises of different metal oxides within their structure with water molecule in the pores or in the voids. A certain loss in mass of zeolite after calcination at about 500°C - 600°C was due to loss of water molecule. Many chemists suggest that for a zeolite material the ratio of silicon and aluminium oxide should be equal and greater than 0.5. The adsorption property, pH value, cation exchange property are some main chemical properties, which depends upon chemical composition of the synthesized nanoporous zeolite materials [22] [23] [24].

### 1.3.3. Ion Exchange and Adsorption Properties

Zeolite having a specific property of cation ($H^+$, $Na^+$, $K^+$, $Ca^{2+}$, $Mg^{2+}$, $Ag^{3+}$, $Zn^{2+}$, $Cu^+$, $NH_4^+$) exchange by the interaction with sorrunding medium during synthesis. However, the cations are balanced by the negative charge developed on the surface of pores of zeolite. This can be attributed to exchange silicon atom by aluminium in some tetrahedra of $[SiO_4]^{4-}$ and converted into $[AlO_4]^{5-}$ tetrahedra, which are connected through each other through common oxygen atom in Figure 1. The heavy metal cations like Cs, Ag, Cd, Pb, Zn, Cu, Hg, Co, Cr, Ni, Ba, Rb, Sr etc. have affanity, zeolite which depends upon hydrated molecular size of the cation and silicon/aluminium molar ratio of the zeolite framework. Due to such properties zeolites have been found good adsorber of gases, liquids materials and separate them for environmental as well as defence purposen [25] [26] [27] [28].

### 1.4. Applications of Zeolites

Zeolites are used as catalyst in many organic reactions like cracking, isomerisation and hydrocarbon synthesis etc. The reaction occurs inside the pores of zeolites, which permit a considerable product authority. Thus zeolites act as oxidation catalysts, acid catalysts as well as shape-selective catalysts as supports for reagents and active metals. Zeolites are greatly used in petroleum refining, synfuels production and petrochemical production [29]. Zeolites can absorb a variety of materials therefore used in variety of applications like drying, purification, separation and also highly used in degradation of toxic compounds and gases like chemical warfare agents (CWAs), volatile organic compounds (VOCs) etc. They can also act as efficient desiccants *i.e.* remove water to very low partial pressures. Zeolites also act as ion exchangers due to presence of loosely bounded hydrated cations which can easily exchange with other cations. Hence zeolites can also be widely used in detergent formulations, nuclear industry, and radioactive waste cleanup and in metal removal applications [30].

### 1.5. Methods for the Synthesis of Zeolites

Most of zeolites present in nature as minerals, and are broadly mined in different parts of the world. Some are synthetic, and are synthesized for specific commercial uses, or synthesized by researchers for understanding the internal chemistry. K. J Murata *et al.* [31] has recommended that zeolites are formed through alteration of rock-water reactions and which changes into sedimentary rock during and after rock formation. Such reactions are also responsible for the production of other minerals. This transmutation of volcanic spoilage leads to the formation of zeolites in layers structures ("zeolite zones") called facies. To determine the types of zeolite formed are carried out by various factors. There are many methods for the synthesis of zeolites. Organic templates used in the synthesis of zeolites are generally toxic and expensive. Therefore, green methods or sustainable methods are applied in the synthesis of zeolites. Green methods [32] include ionothermal synthetic method (by using ionic liquids as solvent),

solvent free synthetic method (water as solvent is completely avoided) [33]. It was found that particle size was much larger than the sizes obtained via the conventional hydrothermal route [34] and relative high efficient zeolites are synthesized through microwave assisted method [35] (homogeneous heating) and hydrothermal method (high pressure) [36]. Thus, among all the methods mention above hydrothermal method is effective, cost effective, easiest and adopted by IZA (International Zeolite Association).

**Hydrothermal method:** Conventional hydrothermal synthesis of zeolites involves heating the reaction mixture in a polytetrafluoroethylene (PTFE) lined steel autoclave (Figure 2).

The safety of the equipment is always of concern due to high autogenous pressure. The hydrothermal synthesis of zeolites sometimes takes long times (1 - 20 days) even at relatively temperature (80˚C - 200˚C), therefore considered as high energy cost process.

## 1.6. Description of Some Selected Zeolites

- Zeolite Beta;
- Linde Type L;
- ZSM-22.

Zeolite beta consists of an intergrowth of two distinct structures termed Polymorphs A and B. The polymorphs grow as two-dimensional sheets and the sheets randomly alternate between the two. Both polymorphs have a three dimensional network of 12-ring pores [38]. Linde Type L (LTL) is one dimensional 12-membered ring channel system has shown as promising material in environmental and industrial applications [39]. ZSM-22 is the member of medium-pore zeolite family (mordenite family) which also includes ZSM-35, ZSM-11and ZSM-5. Almost all members of this zeolite family consist five-membered rings with curvy channels enclosed by ten-membered rings. The free diameter of groove of the channel is ~0.45 × 0.55 nm. The growth of channel was observed in single face direction and having no criss-crossing of the channels [40].
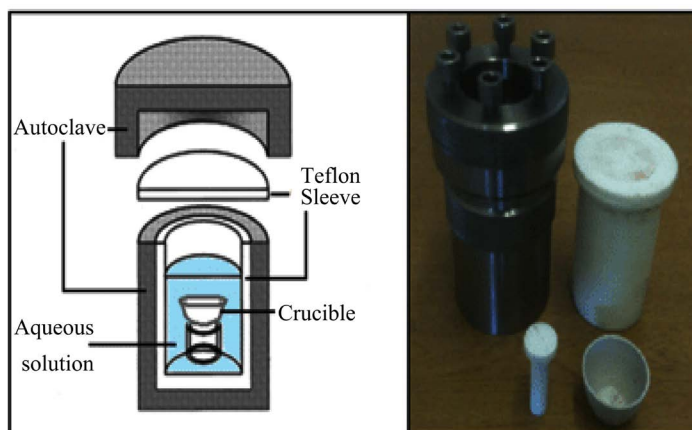


**Figure 2.** Showing schematic diagram of autoclave [37].

## 2. Chemical Warfare Agents

Chemical warfare agents (CWA) are chemical substances that are used in warfare or terrorist activities to kill or seriously injure the people though their physiological effects [41]. A German scientist named Gerhard Schrader accidentally discovered the first nerve agent, Tabun in 1930. With the passes of time many other stable nerve agents have been developed by mid of 1950 and this is known as V-agent in USA nomenclature. Tabun is very poisonous among all toxic substances ever synthesized [42]. Similarly sulfur mustard ($C_4H_8Cl_2S$) is one of a class of chemical warfare agents known as vesicants because of their ability to form vesicles, blisters on exposed skin. The odor of nerve agent like mustard or garlic, hence it gets its common name sulfur mustard. The first use of nerve agent in war was by Afghanistan in 1979-80 and Iraq-Iran war from 1984-1987. The resulting Iraq-Iran chemical warfare was estimated more than 50,000 casualties. Immediately after the war, researchers were totally focused on studies of nerve agent CWA and their mechanisms. Efforts were made to discover new effective methods of protection against these CWA and its simulants [43] [44] [45] [46]. Table 3, describes an overview of all above mentioned toxic chemical warfare agents along with their symptoms method of exposure and toxic manifestations. CWA's have been used at least twelve conflicts since including the first Iran-Iraq war know as Persian Gulf War. In Table 4, we mentioned some major chemical attacks and estimated value of casualties. Although a number of national and international convention have banned the development, production and stockpiling of chemical weapons. In spite of this, these toxic chemicals are still used.

**Table 3.** An overview of CW agents [47] [48] [49].

| Type of Chemical Warfare Agent | Class of Chemical Warfare Agent | Toxic Manifestation | Exposure Method | Symptoms |
|---|---|---|---|---|
| Blister agents | HD, HN1 HN2, HN3, L1 | Slow Fast | Inhalation | Acute; Eye, Skin and Lung Damage, Rash Skin Blistering |
| Nerve agents | GB, GA, GD, GF, DF, VX and RVX | Fast | Inhalation | Sludge, Miotic, Pupils, Weakness, Muscle Spasms, Flaccid Paralysis, Seizures, Shortness of Breath Respiratory Failure, Vomiting and Diarrhea |
| Blood agents | CK, AC | Fast | Inhalation, Skin Absorption, Ingestion | Hypotension, Cyanosis, Severe Distress, Cardiac Arrest |
| Choking agent | CG CL, PS | Slow Fast | Inhalation, Skin Absorption, Ingestion | Serve Pain in Expose Area, Hyperkalemia, Vomiting, Gastrointestinal Distress |

Table 4. Chemical warfare agents as chemical weapons in wars and estimated causalities [50] [51].

| Name of Country | Year | CWA | Causalities (Estimated) |
|---|---|---|---|
| Germany | 1915-18 | Chlorine, phosgene and Mustard gas | 120,000 |
| Italy | 1936 | Mustard gas | 15,000 |
| Japan (Two Times) | 1937-45 and 1995 | Mustard gas | 2500 |
| America | 1962-1967 | Tear gas and Herbicides | 2000 |
| Afghanistan | 1979-80 | Mustard gas | 2100 |
| Iraq | 1980-88 | Mustard gas | 50,000 |
| Syria (Four Times) | 2013-18 | Sarin gas | 1000 |

Therefore Chemical Warfare Agents (CWAs) are very toxic compounds basically used to kill, injure or harm people as well other living organisms. They are also hazardous to the environment (*i.e.* contaminate air, water and land). Hence, there is increasing interest in the effective detection as well as degradation of these compounds [52].

## 2.1. Classification of Chemical Warfare Agents

The CWAs have different characteristic property and thus belong to different categories with distinct physicochemical properties. Thus, they are classified in many ways [53] discussed as follow.

### 2.1.1. On the Basis of Volatility, They Are Classified into Two Categories

- **Persistent agents:** The less volatile agents *i.e.* persist in the environment for longer duration like sulfur mustard (HD) and VX come under this category.
- **Non-persistent agents:** The more volatile agents (evaporated quickly) are known as non-persistent agents like chlorine, phosgene and hydrogen cyanide.

### 2.1.2. On the Basis of Chemical Structure, They Are Classified as Follows

- **Organophosphorus (OP):** G-nerve agents such as Tabun (GA), Sarin (GB), Soman (GD), Cyclosarin (GF) etc.
- **Organosulfur:** HD or Sulfur mustard.
- **Arsenicals:** Ethyldichloroarsine (ED), Methyldichloroarsine (MD), Phenyl-dichloroarsine (PD) and 2-Chlorovinyldichloroarsine etc.

### 2.1.3. On the Basis of Physiological Effects (Harmful/Lethal Effects) by the CWAs, These Can Be Classified into Following Categories

- **Psychomimetic agents:**

Psychomimetic agents also called psychotogenic agents which cause delusions and hallucinations on exposure. Opioid drugs and hallucinogenic drugs come

under this category [53].

- **Nerve agents (highly toxic):**

As the name suggests they affect the nervous system functioning. These agents belong to group of Organophosphorus (OP) compounds. The first known nerve agent, Tabun (GA) was developed as new OP insecticides. This nerve agent series is known as the G-agents, which include Sarin (GB), Cyclosarin (GF) and Soman (GD). Then, V-agents were developed which were more stable derivatives of G agents. VX (a sulfur-containing OP) is more stable, less volatile and less water-soluble, acting through direct skin contact, and persisting in the environment up to several weeks after release as compared to other G agents. Atropine and Pralidoxime are used as nerve agent antidotes [54].

- **Vesicants (blistering agents):**

These cause blisters or skin injuries. There are two forms of vesicants: mustards (sulfur and nitrogen mustards), lewisites and arsenicals. Sulfur mustard (commonly known as mustard gas, HD, LOST, Yperite, etc.) is called as the king of CW agents. Few examples of vesicants with their chemical formula are: [55]

- Sulfur Mustard (HD) $ClCH_2CH_2SCH_2CH_2Cl$;
- Nitrogen Mustard (HN-1) $(CH_2CH_2Cl)_2NC_2H_5$;
- Nitrogen Mustard (HN-2) $(CH_2CH_2Cl)_2NCH_3$;
- Nitrogen Mustard (HN-3) $N(CH_2CH_2Cl)_3$;
- Lewisite (L) $ClCH=CHAsCl_2$.

- **Bloods agents (cyanogenic agents):**

These agents get absorbed into the blood by binding with oxygen-carrying hemoglobin in the blood generally known as "cyanide poisoning", hydrogen cyanide (HCN), cynogen $(CN)_2$, phosgene $(COCl_2)$, arsine $(AsH_3)$, cynogen chloride (NCCl) and cynogen bromide ((CN)Br) come under this category [56] [57].

- **Choking agents:**

Chocking agent's also known by the name pulmonary agents. Chlorine gas $(Cl_2)$, chloropicrin (PS) $(Cl_3CNO_2)$, diphosgene $(ClCO_2CCl_3)$, disulfur decafluoride $(S_2F_{10})$, perfluoroisobutene $(C_4F_8)$ etc. are some comman examples of such agents. Throat burning, headache, coughing, vomiting, chest pain are major symptoms on inhalation of these agents [58] [59] [60].
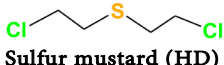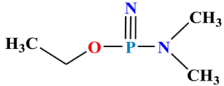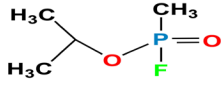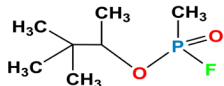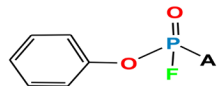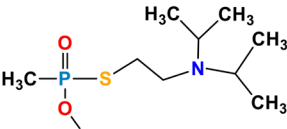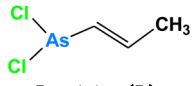
- **Riot-control agents:**

Riot control agent's also known by another name called lachrymatory agents or tear gases. The symptoms of these agents are skin & eye irritation, respiratory, Chest pain, vomiting and even blindness. Capsaicin, CS gas $(C_{10}H_5ClN_2)$, CR gas (dibenzoxazepine), CN gas (phenacyl chloride), bromoacetone etc. are some comman examples of such agents [61] [62].

## 2.2. Molecular Structure of CWA

Molecular structure of some CW agents is given in Table 5, along with IUPAC name, common names and percentage of each atom in particular CW agent.

**Table 5.** Molecular structure, IUPAC and common name of CW agents.

| Structure of CW Agents | IUPAC Name & Composition (%) of Atoms | Common Names |
|---|---|---|
| **Sulfur mustard (HD)** | 1-chloro-2-[(2-chloroethyl)sulfanyl]ethane<br>C (30.20%), H (5.07%), Cl (44.57%), S (20.16%) | Mustard gas |
| **Tabun (GA)** | EthyN,N,dimethyl phosphoramidocyanidate<br>C (41.10%), H (7.59%), N (19.17%), O (10.95%), P (21.20%) | Tabun |
| **Sarin (GB)** | Propanyl methylphosphonofluoridate<br>C (34.29%), H (7.19%), F (13.56%), O (22.84%), P (22.11%) | Sarin |
| **Soman (GD)** | Propan-2-yl methylphosphonofluoridate-ethane<br>C (42.35%), H (9.48%), F (11.16%), O (18.80%), P (18.20%) | Soman |
| **Cyclosarin (GB)** | Cyclohexylfluorophosphonate<br>C (38.29%), H (3.19%), F (13.56%), O (22.84%), P (22.11%) | Cyclosarin |
| **Amiton (VX)** | S-{2-[di (propan-2-yl)amino]ethyl} O-ethyl methylphosphonothioate<br>C (49.41%), H (9.80%), N (5.24%), O (11.97%), P (11.58%), S (11.99%) | Amiton |
| **Lewisite (L)** | 2-Chlorovinyldichloroarsine<br>C (19.28%), H (2.70%), As (40.09%), Cl (37.94%) | Lewisite |

## 3. Simulants of CW Agents

Chemical warfare agent simulants are less toxic than real agents. These compounds suitable as spectral simulants that give rise to similar spectral characteristics and mimic all the properties of a CWA except for its toxicity. There is recommence interest in the environmental fate of Chemical Warfare Agents attributable to expand threat of chemical weapons use in a terrorist attack. The knowledge acquisition procedures used that influence the providence of Chemical warfare agents such as sulfur mustard, Lewisite, Tabun, Sarin, Soman, VX etc. in the environment are important for evolution of demolition strategies and exposure evaluations. Hence, it is necessary to extremely examine the behavior of Chemical agent by using their simulants because of the toxicity of the agents and diminution. An ideal simulant is the one which shows all the major chemical and physical properties of the CWA without any toxic or lethal properties. No definite simulant is ideal because a single simulant cannot effectively represent

all environmental fate properties of a given CWA. Thus, depending on the concerned physical-chemical property, a number of different chemicals are used as chemical warfare agent's simulants [52] [63] [64]. List of some common simulents are shown in Table 6.

## 3.1. HD Simulants

Sulfur mustards, particularly bis (2-chloroethyl) sulfide (HD) are a well known class of chemical warfare agent (CWA). Pure sulfur mustards are colorless, viscous liquids at room temperature. Sulfur mustards which have the ability to form large blisters on direct contact to skin and in the lungs. Molecular structures of simulents of HD are shown in Figure 3 [53] [64] [65] [66].

## 3.2. G-Agents

Nerve agents are compounds that have the greater potential to inactivate the enzyme acetylcholinesterase (AChE) which is present in nerve system. The first compounds to be synthesized were known as the G-series agents ("G" stands for German): tabun (GA), sarin (GB) and soman (GD). The organophosphate nerve agents GA, GB, GD, and GF are found very volatile in nature and having most toxic nature. Simulants molecular structures are shown below (Figures 4-6) [6].

**Table 6.** Some common simulents of CW agents.

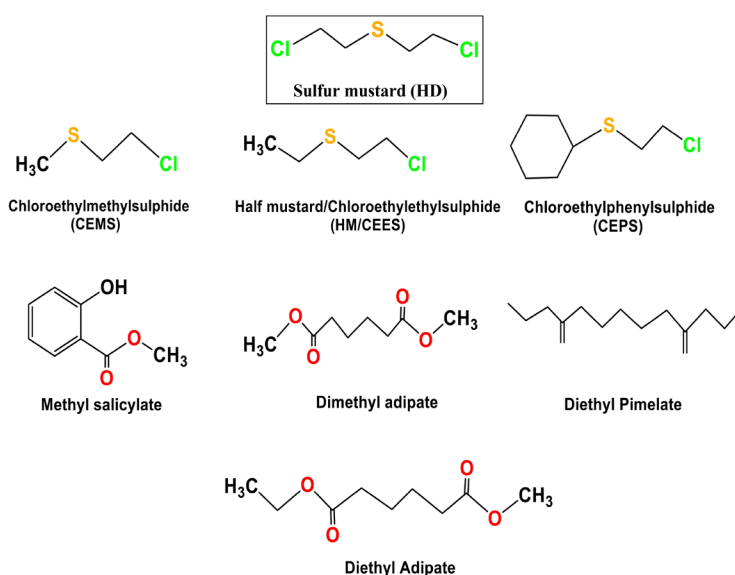| S. No. | Simulant | Type of CWAs |
|--------|----------|--------------|
| 1. | CEES, CEMS, CEPS | HD (Blistering agent) |
| 2. | DPDP, DMMP, DEEP, TEP, DIMP, TMP | G (nerve agent) |
| 3. | Amiton, DEPPT, Malathion, Parathion | V (nerve agent) |
| 4 | Lewisite Oxide , Phenyl arsine oxide | Lewisite (L), Blistering agent |



**Figure 3.** Molecular structures of HD stimulants.

## 3.3. VX-Agents

The V-series agents are class of the group persistent agents, which have low volatility and can remain on skin, clothes, and other surfaces for long periods of time. The consistency of these nerve agents is very much similar to oil and this consistency renders them toxic mainly by dermal exposures. The other agents in the V-series are less known, and the information available about their characteristics is fairly limited in the open, unclassified literature. The other agents also have coded names; including VE, V-gas, VG and VM. Molecular structures are shown in **Figure 7** [64] [67].
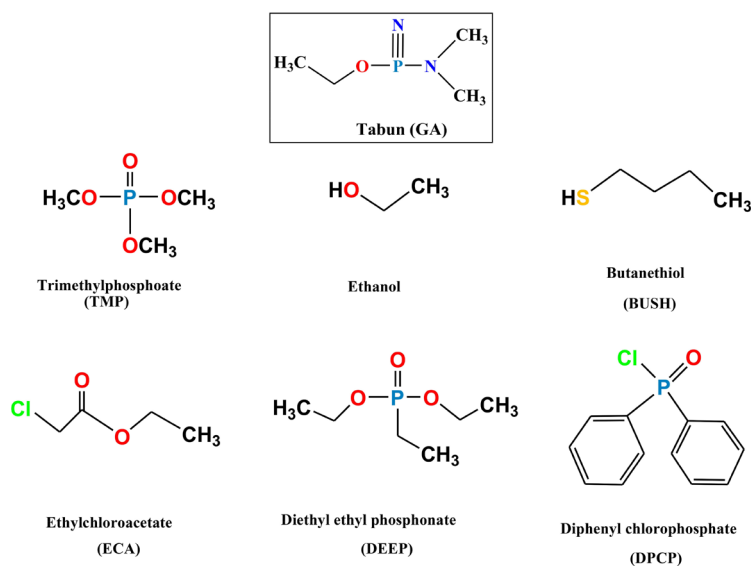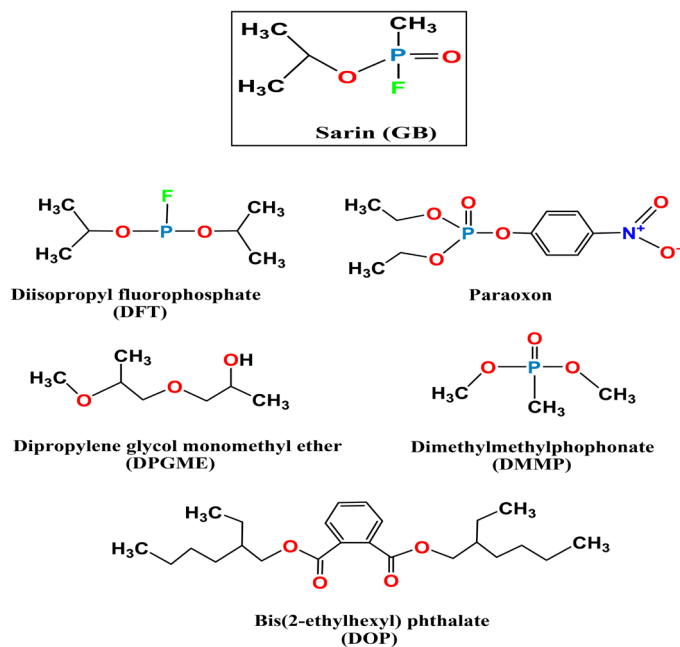
**Figure 4.** Simulants of tabun (GA).

**Figure 5.** Simulants of sarin (GB).
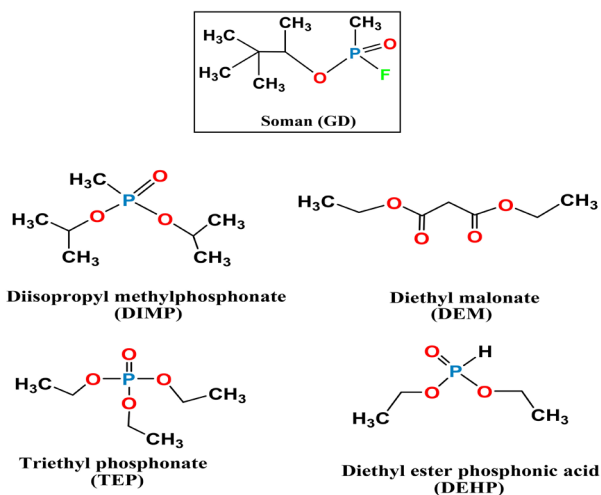
**Figure 6.** Simulants of soman.
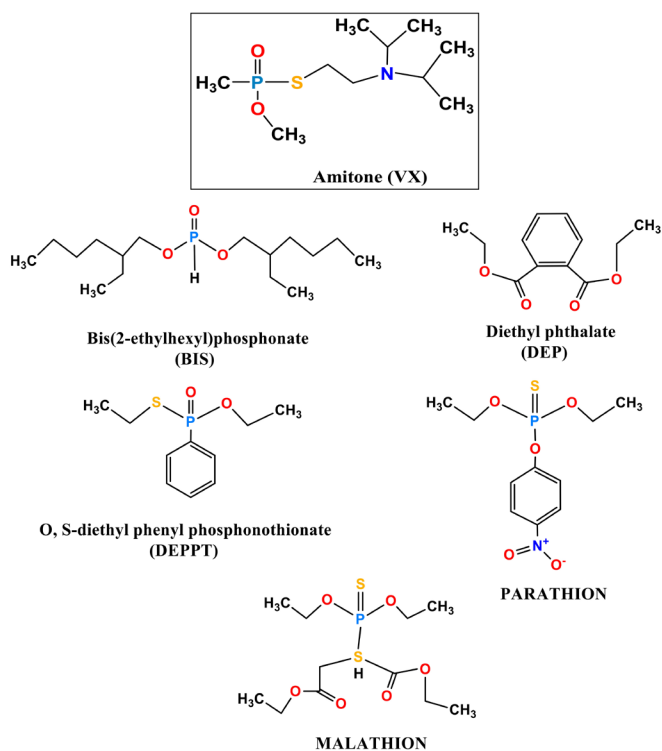


**Figure 7.** Simulants of amitone.

## 3.4. L-Agents

Lewisites (L) are Organoarsenic compound and known blister agent and lungs irritant. The Lewisite made as a war gas in 1918 by W. Lee Lewis. It was manufactured in Germany, Japan, US, and the Soviet Union for use as chemical weapon. At room temperature pure lewisite was found more volatile than sulfur mustard. It is colorless oily liquid having "geranium" odor. But the impure lewisites are brown, yellow, violet-black, green, or amber oily liquids. The simulants of lewisite are shown in **Figure 8** [64] [68] [69].

**Figure 8.** Simulants of lewisite (L).

## 4. Physico-Chemical Properties of CWA

Some essential physical and chemical properties of Chemical Warfare Agent are given in **Table 7**, which provides useful information about particular agent. A verity of compounds has been used as simulent for CWA on the basis of their physico-chemical properties.

## 5. Decontamination Methods

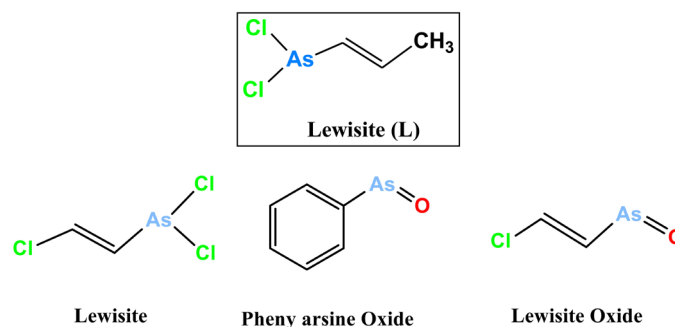Decontamination is a complex process and can be considered in different ways. Some basic fundamental methods of decontamination of chemical warfare agents are physical decontamination, mechanical decontamination, biological decontamination and chemical decontamination (**Figure 9**). Decontamination means a method used to reduce or remove and destroy the toxic nature of chemical agents [72]. Different CWAs are degraded by different chemical processes [73].

HD gas is degraded by dehydrohalogenation (CaO have this property and thus used against the degradation of CEES), aerobic oxidation by the help of catalyst [74], oxidation by using hydrogen peroxide, photo oxidation (TiO$_2$ have this property). G agents are degraded by two methods: enzymatic hydrolysis and non-enzymatic hydrolysis. In enzymatic hydrolysis organophosphorous hydrolase enzyme (microbial degradation) is involved [75]. Such catalyst yields large amount of acidic products therefore buffer is required to maintain the pH of the reaction in neutral to slightly alkaline range [76]. Non-enzymatic hydrolysis involves chemical compounds (*i.e.* iodosylcarboxylates) that promote catalytic hydrolysis in which nucleophilic substitution and hydrolysis reaction takes place [77].

## 6. Zeolites and Composites of Zeolite Used for Decontamination of CWA and Its Simulants

A survey of literature revealed that zeolites and composite of zeolites play an important role in the welfare of society and emerged as an important field of research due to their diversified applications as these are completely safe and natural material. A lot of research work has been carried out for the degradation of

chemical warfare agents by different materials (e.g. metal oxides like MgO [52] [78] [79] [80], CaO [81], $Al_2O_3$ [82], ZnO [83], lanthanum oxide and $Fe_2O_3$ [84], $Y_2O_3$ [85], nanorods [86], nanotubes [87] [88], nanobelts [89], detoxifying catalyst and reactive polymers [73] [90]). However, a little effort has been made to synthesize zeolites or its derivatives (doped with either by metal oxides [91] or polymers [92]). This fact has prompted us to synthesize some new metal oxide doped zeolites for the degradation of CWAs.

## 7. Literature Survey

F. Carniatoa *et al.* [93] (2018) have been reported a class of heterogeneous naturally originated and commercially available catalysts bentonite which contain at least 80 wt% of montmorillonite clay. It was designed selectively transform toxic organosulfur and organophosphorus CWAs into non-toxic products at mild conditions and shows negligible effect on health as well as on environment. It was also performed oxidative abetment of 2-chloroethyl ethyl sulphide (CEES), well known simulant of HD in presence of $H_2O_2$ as an oxidant. Furthermore decontamination formulation was studied by mixing sodium perborate as an oxidant with iron bentonite. This study conceded a good decontamination test surface among CWAs and about 80% contaminated degradation within 24 hours under ambient conditions.
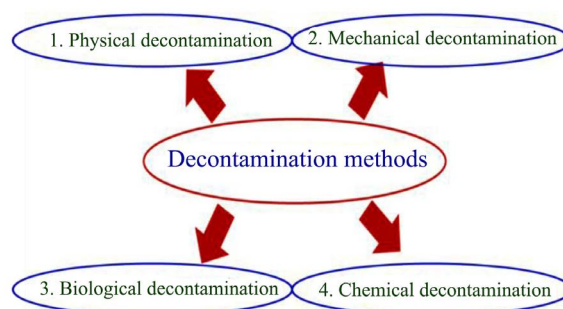


**Figure 9.** General methods of decontamination.

**Table 7.** Physico-chemical properties of CWA simulants [55] [64] [70] [71].

| Acronym of CWA | V.p* (mmHg) at 25˚C | F.p* (C) ±2 | B.p* (C) ±2 | V.d* (air = 1) | M.W* (g/mol) | Volatility (mg/m³) at 25˚C | P.s* at 20˚C | Persistency |
|---|---|---|---|---|---|---|---|---|
| HD | 10 | 14.45 | 218 | 5.5 | 159.07 | 906 | liquid | Persistent |
| GA | 0.057 | −50 | 248 | 5.6 | 162.13 | 497 | liquid | Non-persistent |
| GB | 2.48 | −56 | 158 | 4.8 | 140.10 | $1.8 \times 10^4$ | liquid | Non-persistent |
| GD | 0.40 | −42 | 198 | 6.33 | 182.17 | $3.9 \times 10^2$ | liquid | Non-persistent |
| VX | 0.0009 | −51 | 292 | 9.2 | 267.37 | 10.5 | liquid | Persistent |
| L | 3.46 | −1.2 | 196 | 7.1 | 207.32 | 3860 | liquid | Persistent |

V.p* = Vapour pressure, F.p* = Freezing point B.p* = Boiling point, V.d* = Vapour density, M.W* = Molecular mass, P.s* = Physical state.

S. Abdul Majid *et al.* [94] (2018) reported sorption efficiency of mordenite versus zeolite-A on nitrate and phosphate. Sorption experiments were investigated between $KH_2PO_4$, $NH_4NO_3$ on surface modified zeolite-A and mordenite. For sorption study batch equilibrium method was adopted. Experiment was performed at a range of pH 3, 5, 7, 9 and 11. The results obtained after investigation suggested that the sorption increases with increase in pH values from 3 to 7 and the equilibrium was attained after about 12 hs. It was also found that the sorption percentage increases when the temperature is raised up to 40. Theoretical studies have also implored for mordenite and results are compared with experimental data which helps to explain the respective relation with sorption capacity and efficiency of the ions.

Y. Liu *et al.* [95] (2018) the detoxification ability of flexible and breathable poly (*m*-phenylene isophthalamide) (PMIA) loaded with MgO nanoparticles was demonstrated by gas GC-MS. They found that after 20 h of reaction time approximately 70.56% of the mustard gas surrogates have been decomposed.

M. Florent *et al.* [96] (2017) reported an investigation on removal of chemical warfare agent (CWA) surrogates by highly porous carbon textiles. The surface morphology of modified carbon cloths was studied and found that the modified materials has capabilities to remove 2-chloroethyl ethyl sulfide (CEES) and diethyl sulfide (EES), two sulfur mustard gas simulants. The experiment was performed in vapor phase, which might be the circumstances of the real life arrangement of mustard gas. For investigation of reaction was carried out by FTIR, XRD, nitrogen adsorption isotherm, BET, potentiometric titration, TGA and GC-MS techniques. The degradation of CEES through hydrolysis and EES is adsorbed in the nylon's amides framework network.

Li Jixiang *et al.* [97] (2017) reported novel efficient and cost-effective magnetic polymer composite macro particles with highly porous activated carbon carrier adsorbent (CsFeAC) was synthesized by using the sol-gel method. It was found that synthesized polymer composite have higher specific surface area and lower crystalinity which enhance the absorption capacity. Due to its higher capacity of adsorption towards $Cu^{2+}$ ions present in water causes a serious threat to the environment and human beings. In this study it was found the adsorption data match better with the Langmuir adsorption isotherm and it shows adsorption is a monolayer adsorption. Furthermore, kinetics studies show that the adsorption adopts the pseudo-second order kinetics.

M. Sadeghi *et al.* [98] (2016) in this study, zinc oxide nanoparticles (ZnO NPs) have been surveyed to decontaminate the chloroethyl phenyl sulfide (CEPS simulent of sulfur mustard) as a sulfur mustard agent simulant. Prior to the reaction, ZnO NPs were successfully prepared through sol-gel method in the absence and presence of polyvinyl alcohol (PVA). PVA was utilized as a capping agent to control the agglomeration of the nanoparticles. The formation, morphology, elemental component, and crystalline size of nanoscale ZnO were certified and characterized by SEM/EDX, XRD and FT-IR techniques. The proposed mechanism is given in Figure 10.
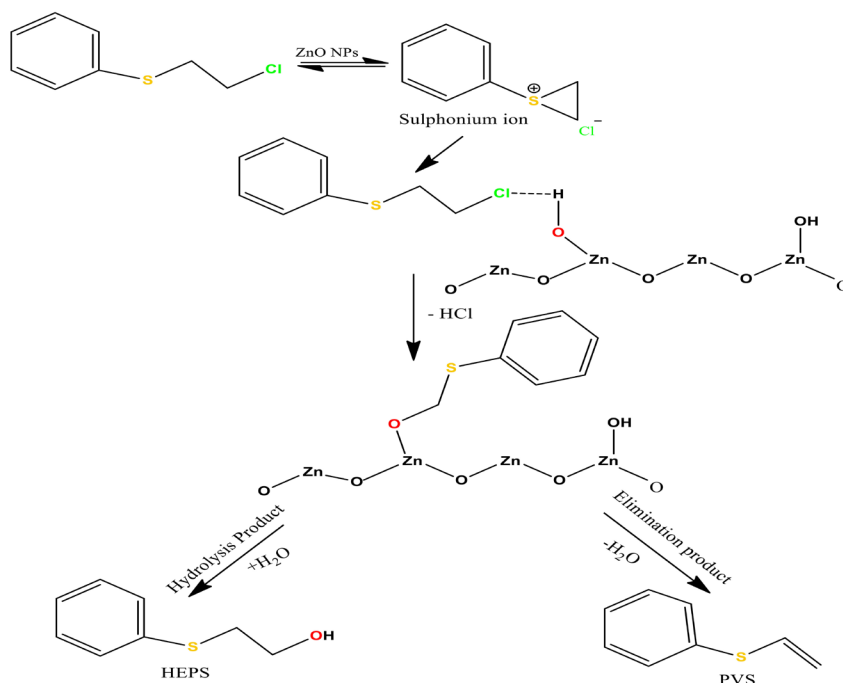
**Figure 10.** Decontamination mechanism of CEPS with ZnO NPs.

M. St'astny *et al.* [99] (2016) used manganese (IV) oxide for degradation of toxic organophosphorus compounds which was prepared by homogeneous hydrolysis of $KMnO_4$ with 2-chloroacetamide. The degradation efficiency was determined with parathion methyl using HPLC and for comparative study, synthesized manganese (IV) oxides by direct method (reaction of $MnSO_4 \cdot H_2O$ and $KMnO_4$, and reaction of $KMnO_4$ with urea in aqueous solution). The sample of $KMnO_4$ with 2-chloroacetamide showed the greatest degradation efficacy of about 90% within 2 h. Reaction mechanism shown in Figure 11.

M. Sadeghi *et al.* [100] (2016) have been reported the performance of NiO NPs/Ag-clinoptilolite zeolite as a novel composite adsorbent for the decontamination of two most known sulfur mustard (nerve agent) simulants 2-chloroethyl ethyl sulfide (CEES) and dimethyl methyl phosphonate (DMMP). The reactions were carried out in both methanol and *n*-hexane solvents and monitored by GC-FID, 31P-NMR and GC-MS analyses subsequently. Moreover, the SEM/EDAX, XRD and FT-IR techniques were applied for characterization of prepared samples. The GC-FID results reveal that the composite material (NiO NPs/Ag-clinoptilolite zeolite) in normal hexane solvent shows excellent 86% decontamination in 12 h at room temperature toward CEES and 31P NMR data reveals that more than 89% decontamination of DMMP within 8 h was found at similar conditions. The calculated value of rate constant and half-life for CEES and DMMP was found $3.8194 \times 10^{-5}$ s$^{-1}$, $7.3055 \times 10^{-5}$ s$^{-1}$ and $1.8640 \times 10^4$ s$^{-1}$, $9.4860 \times 10^3$ s$^{-1}$ respectively. The product formed during hydrolysis *i.e.* hydroxyl ethyl ethylsulfide (HEES) and methyl phosphoric acid (MPA) was recognizing by GC-MS analysis.
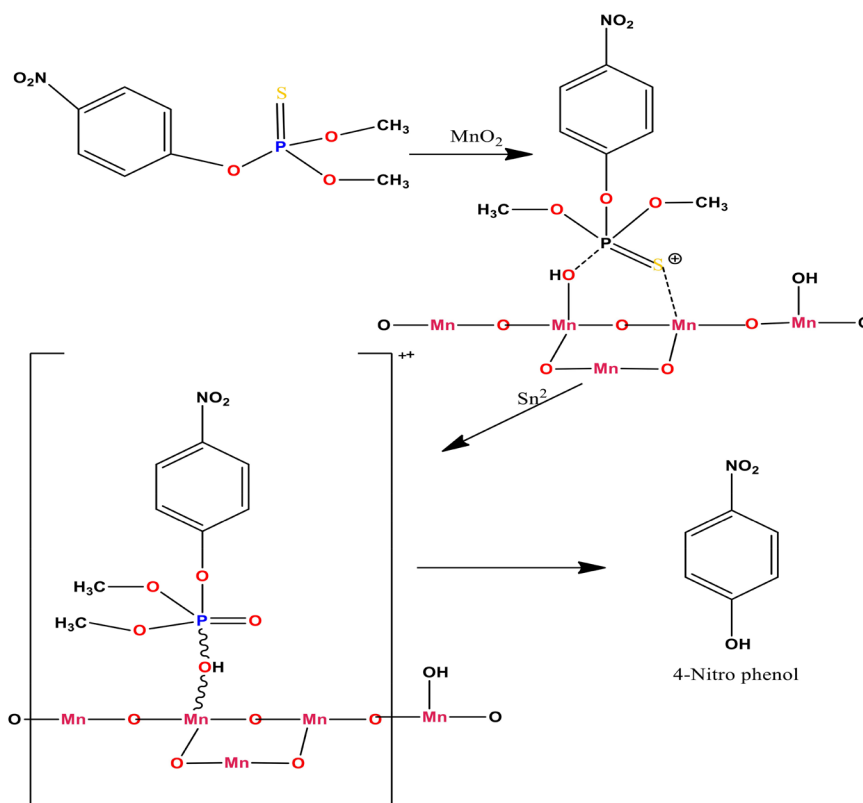
**Figure 11.** Degradation mechanism of parathion methyl by mesoporous $MnO_2$.

**A. Hiromichi *et al.* [101] (2016)** reported synthesis of mordenite zeolite and its composite material using for toxic Cs ion decontamination. Reagents $SiO_2$ and $NaAlO_2$ used for synthesis without addition of a template and a seed powder. In this reaction, obtained mordenite contains Al/Si ratios 0.085:0.120 was found, at temperature range between 170°C to 200°C for 24 h. Initially Mordenite zeolite (1.0 g) show greater than 99% and 85% - 92% adsorption capacity for 100 ppm $Cs^+$ (100 mL) solutions of water and seawater respectively. The $Cs^+$ cation exchange capacity was found 180 - 210 cmol kg (centi moles of charge per kilogram) and it increases with varying Al/Si ratio. Furthermore for the magnetic collection composite material of the mordenite and magnetite of 10, 20 and 30 wt% was synthesized and tested for decontamination. It was observed that total $Cs^+$ ion decontamination rates were also high (more than 95%) by using the magnetic collection material after the $Cs^+$ adsorption in water. Mordenite zeolite has been found very effective adsorbent for radioactive $Cs^+$ ion decontamination because of high selectivity. The cation exchange capacity and the $Cs^+$ adsorption ability in seawater was found in good agreement compared to the synthesized mordenite from diatomite and the natural mordenite because of the low impurities for the material made from the chemical reagents.

**K. Dastafkan *et al.* [102] (2015)** reported 20 wt% $MnO_2$NPs-AgY zeolite catalysts in different solvents for decontamination reactions of O,S-diethyl methyl phosphonothiolate (OSDEMP), as an agricultural organophosphorus pesti-

cide. This reaction was studied by GC-FID and GC-MS techniques. The catalyst was synthesized in three different steps: in first step, Na-Y zeolite was prepared by hydrothermal method. In second step, by using ion exchange procedure Ag-Y zeolite was prepared from Na-Y zeolite. In final step, $MnO_2NPs$ were synthesized by doping of Ag-Y zeolite into manganese (II) nitrate solution. The confirmation of the synthesized material and nanocomposite catalyst was characterized through SEM, XRD, AAS and FTIR spectroscopy techniques. In this study it was found $MnO_2NPs$-AgY zeolite composite catalyst (20 wt%) has capacity to convert OSDEMP into a less toxic or non-toxic product. Adsorption, degradation and hydrolysis reactions were studded in different solvents and time intervals at normal temperature and pressure conditions. The procedure for reaction was given in Figure 12 and reaction mechanism is shown in Figure 13. This study concludes synthesized 20 wt% $MnO_2NPs$-AgY zeolite nanocomposite has greater decontamination efficiency towards OSDEMP molecule and it was also found that OSDEMP molecule was perfectly decontaminated (100%) in n-heptanes solvent after 8 hours.

V. V. Singh *et al.* [103] (2015) reported CWAs (diethyl chlorophosphate) and BWAs (against *E.* coli bacteria) detoxification by using silver-exchanged zeolite (AgZ) micromotors. Such multifunctional reactive Ag-zeolite micro-motors are highly efficient on-the-fly for detoxification strategy of chemical and biological threats under ambient conditions. The synthesized new Ag-zeolite micro motor was very much effective towards detoxification of CWAs. The combination of Ag-zeolite micromotors catalyst reflects effective adsorption capacity due to embedded $Ag^+$ ion and the dynamic moment behavior of the micro motors. The synthesized Ag-zeolite micro motors have a specific function and its components are useful practically sustainable, economical, and eco-friendly. All the studies clearly indicated that the presence of micropores and high surface area of the zeolite facilitate the adsorption of DCP molecules within it. Also the presence of $Ag^+$ (also have antibacterial activity) leads to stronger interactions and accelerated chemisorptions process. The mechanism of this process is shown in Figure 14. These properties and capabilities of zeolite micro motors make it advantageous over recently developed motors and lead to detoxification and to green degradation products.

J.P. Kumar *et al.* [104] (2015) synthesized and compared degrading ability (HD gas) of eight different metal oxides (*i.e.* MgO, CaO, NiO, CuO, $Ag_2O$, $MnO_2$, $CeO_2$ and $Fe_2O_3$) and doped with 13-X zeolite. Zeolites were characterized by the help of XRD, TEM and SEM-EDAX while the decontamination reactions were studied by the help of GC and GC-MS. TEM images depicted different shapes of various $MO_X$-13X materials. Nanorods in case of NiO-13X while nanobelts in $MnO_2$-13X and MgO-13X. XRD graph patterns showed no changes in crystal structure of zeolite by doping with metal oxides. It was also found that surface area has decreased after doping with metal oxide nano-particles and shows better reactivity against decontamination of HD. This is due to blocking of micropores which cause the decrease of micropore volume. The data in Table

8 shows decontamination efficiency. Maximum efficiency was shown by Ag$_2$O-13X which degraded 100% of HD gas in 16 h.

**Table 8.** List of Nanoparticals used as decontamination material.

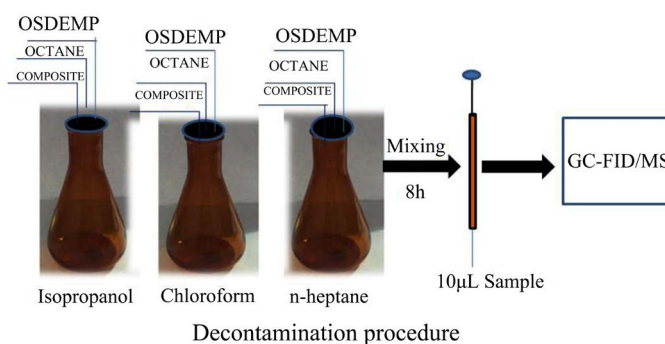| Synthesized Nanoparticles | Time | Decontamination of HD (%) |
|---|---|---|
| CaO-13X, MnO$_2$-13X, MgO-13X | 48 h | 100 |
| NiO-13X | 48 h | 95.8 |
| CeO$_2$-13X | 48 h | 94.5 |
| CuO-13X | 48h | 94.3 |
| Fe$_2$O$_3$-13X | 48 h | 92.2 |
| Na-13X | 48 h | 66 |
| Ag$_2$O-13X | 16 h | 100 |



**Figure 12.** Synthetic process of NaY and AgY zeolite and MnO$_2$NPs-AgY nanocomposite along with the decontamination process.
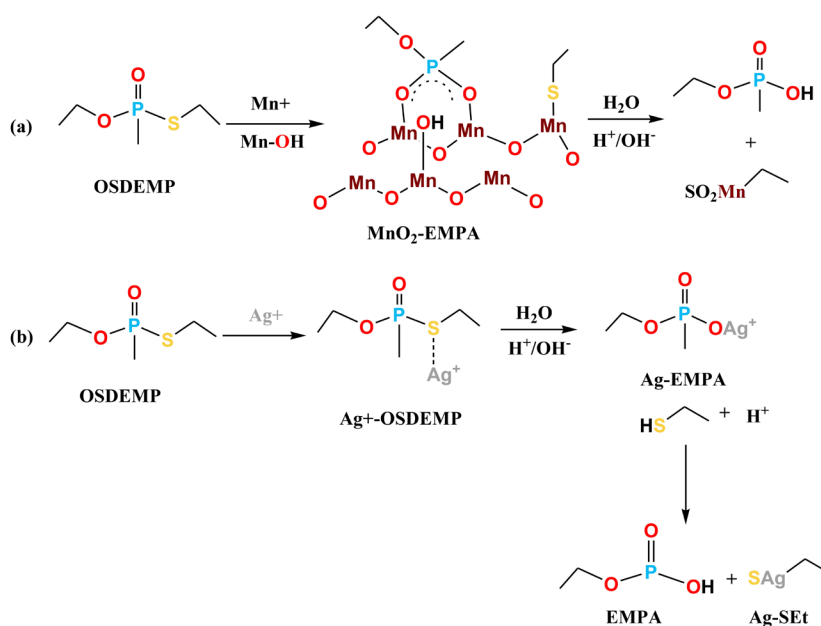


**Figure 13.** Proposed reaction mechanism of the decontamination of OSDEMP on the surface of the 20 wt% MnO$_2$NPs-AgY zeolite; (a) Manganese and (b) Silver as reaction site.
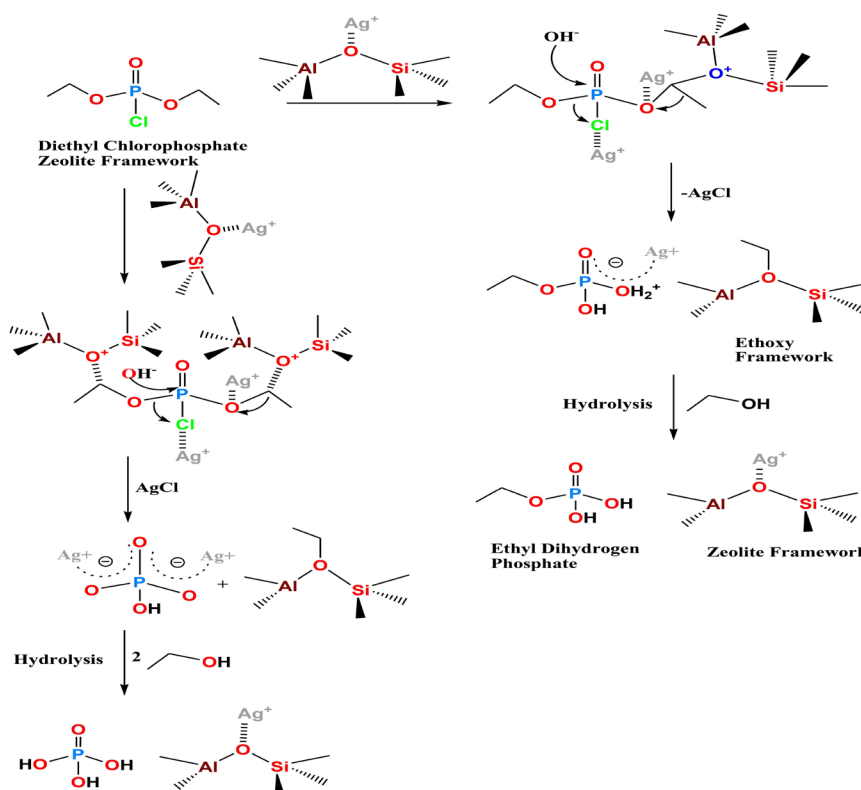
**Figure 14.** Reaction mechanisms for the hydrolytic conversion of DCP into hydrolytic products on Ag-Z micromotors.

This unusual efficiency of silver oxide has been explained. Silver ion abstracts chloride ion from HD gas and thus convert it into its degraded products. It was found that silver ion possess relatively higher affinity towards sulfur atom of HD as compared to other metal ions. GC-MS has confirmed that on bare Na-13X zeolite only hydrolysis reaction takes place on its surface while in $MO_X$-13X materials have elimination as well as hydrolysis reactions. Reaction of HD on Na-13X results the formation of HM (hemisulfur mustard) and TDG (thiodiglycol) products. While on reaction with $MO_X$-13X materials, six different products (1,4-oxathiane, chloroethyl vinyl sulfide, hydroxyl ethyl vinyl sulfide, HM, TDS and divinyl sulfide) were formed. Proposed mechanism is shown in **Figure 15**.

**M. Sadeghi *et al.*** [91] **(2014)** have synthesized $MnO_2$-AgX zeolite nanocomposites. It was a novel adsorbent catalyst for the decontamination against 2-CEPS and 2-CEES (sulfur mustard simulants). The reaction mechanism for the decontamination of Sulfur mustard simulants are shown in **Figure 16(a)** and **Figure 16(b)**. Crystalline size and morphology were explained with the help of SEM, AAS, GC-FID, GC-MS and GC analysis. Above characterization techniques reveals that the amounts of silver (10.3 wt%) and manganese (18.4 wt%) were sufficient for complete decontamination (100%) within 12 h and changes these toxic simulants into non toxic products.
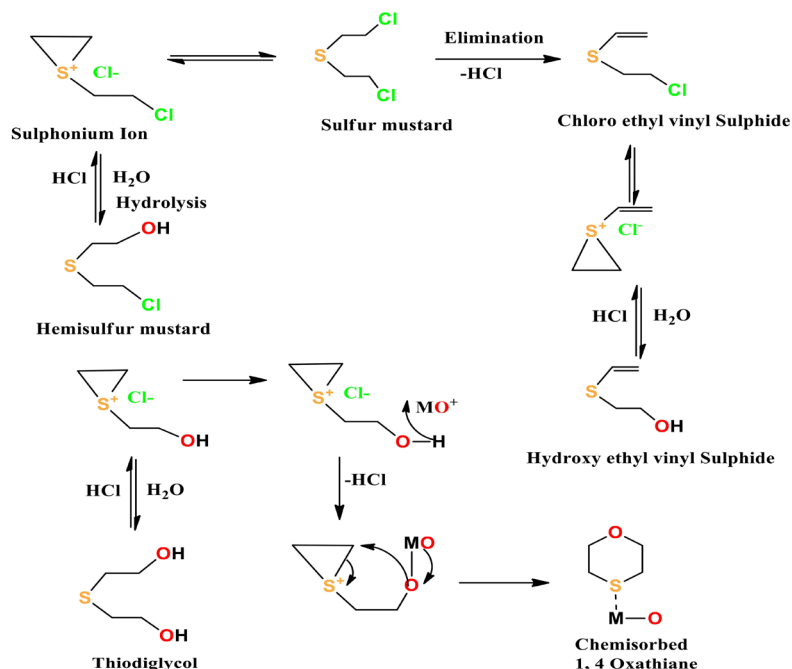
**Figure 15.** Proposed mechanisms for decontamination of CWA simulants with doped zeolite.
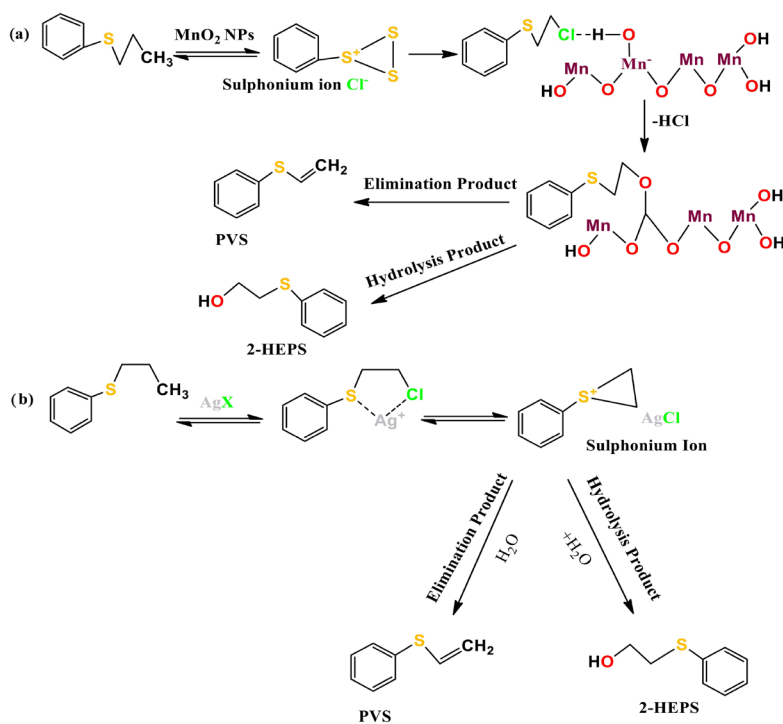


**Figure 16.** (a, b) Reaction mechanism for the decontamination of 2-CEPS and CEES.

**W. A. Khanday *et al.* [105] (2014)** reported the adsorption of dimethyl methyl phosphonate (DMMP) over synthetic zeolite-*α*. It was observed that initially adsorption of DMMP was found to be high and then it decreases with an increase in the injection volume. Thus adsorption rate was increases with in-

crease in the contact time between zeolite-*α* and DMMP. The reaction mechamism is shown in **Figure 17**. Zeolite-*α* shows equilibrium time up to 8 h and after reaching equilibrium, the adsorption rate become almost constant. Further desorption experiment was performed and completed successfully the data demonstrate that desorption exhibit from both strong and weak adsorption sites.

**W. A. Khanday *et al.* [106]** (2013) have been reported that Zeolite-A, Zeolite-X, MCM-22 and Erionite were synthesized by hydrothermal methods and were characterized successfully by X-ray diffraction (XRD), Fourier transform infrared (FTIR) spectroscopy, scanning electron microscopy (SEM), Brunauer-Emmett-Teller (BET) surface area analysis, energy dispersive spectroscopy (EDS) and thermal programmed desorption (TPD). The adsorption of dimethyl methyl phosphate (DMMP) was performed on these synthesized zeolites. The adsorption data demonstrated that highest surface area among all zeolites was shown by Zeolite-X and having highest adsorption capacity followed by Erionite and MCM-22 whereas Zeolite-A shows the least surface area and having least adsorption capacity. On comparing the surface area of synthesized zeolite the order of increasing surface area was found: Zeolite-X > Erionite > MCM-22 > Zeolite-A. In this study it was also found that initially adsorption rate was found to be high for all zeolites and then it decreases with increase in injected volume. Further desorption study was carried out successfully and two types of desorption pattern peaks were observed. The sharp peaks of desorption pattern representing desorption of physisorbed DMMP and broad peaks representing desorption of strongly chemisorbed DMMP. The mechanism of reaction is shown in **Figure 18**.

**S. L. Sharifi Alhashem *et al.* [107]** (2012) have been investigated decontamination of diethyl methyl phosphonate (DEMP,) and 2-chloroethyl phenyl sulfide (CEES) (simulent of Sulphur mustard, HD) by using nano-$MnO_2$/Zeolite AgY composite. It was found that, in first case 2-CEPS was produced about 86% by composite after 24 h, and it changed to less toxic chemical products **Figure 19(b)** and in second case absorption of DEMP was found nearly 87% after 30 h **Figure 19(a)**. Results are identified by GC-MS and proton NMR respectively.

**R. Satya Agarwal *et al.* [92]** (2012) have been reported the detoxification of Paraoxon (simulent of sarin, nerve agent) by functionalized cellulose/ PET polymer/ zeolites (Linde type A and Mordenite). The stimulant paraoxon detoxification studies by functionalized membranes were successfully obtained.

The prepared paraoxon stock solution shows UV absorbance value at 6.8 nm. After adding prepared functionalized cellulose/PET polymer/zeolites fibers to stock solution of paraoxon, a decrease in the UV absorbance value of paraoxon solution was observed within time interval of 15 min and 1 hour. This decrease in the UV absorbance value shows that the catalyst containing nanofibers has the capacity to detoxifying harmful agent like organophosphorous. This concludes, functionalized cellulose/PET polymer/zeolites are tested for the decontamination of nerve agent simulant Paraoxon, and stimulant gets hydrolyzed. The rates of

hydrolysis for different organophosphate hydrolyzing agents are compared and it was found that the reactivity and amount of adsorption of these catalysts are of higher.



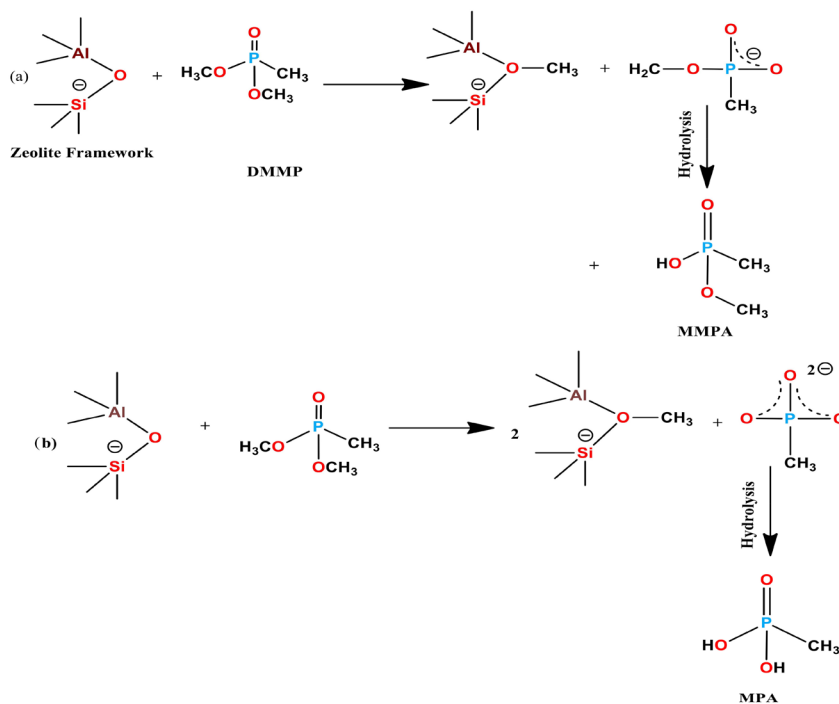**Figure 17.** Mechanisms for the hydrolytic conversion of DMMP into MMPA and MPA on zeolite framework.
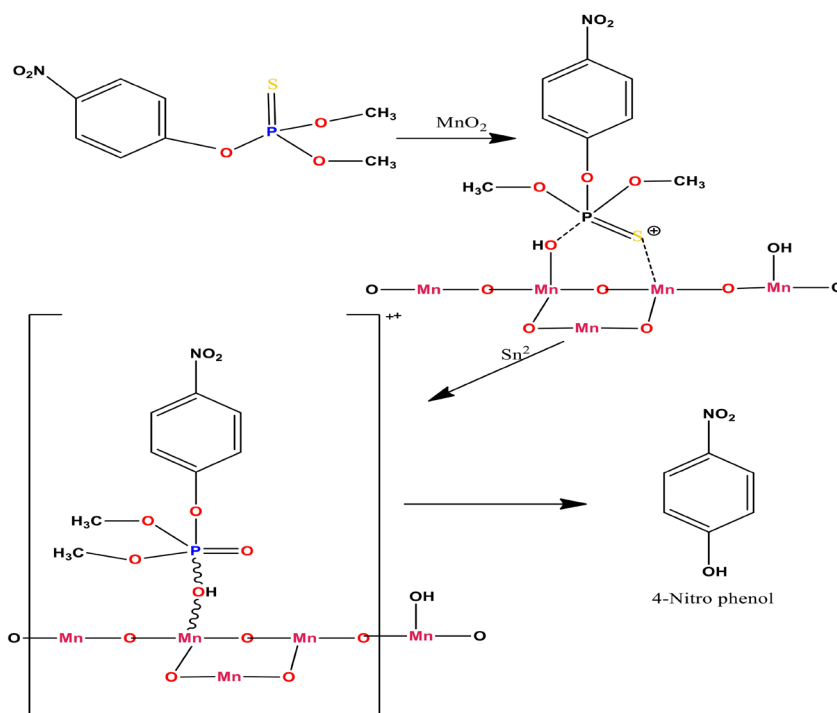


**Figure 18.** Decontamination process of zeolite towards substituted DMMP.
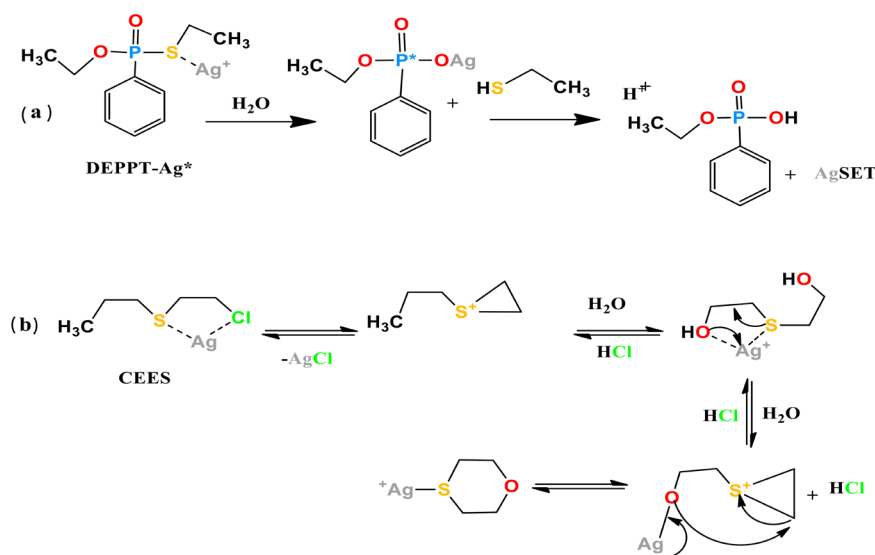
**Figure 19.** (a, b) Reaction mechanisms for the decontamination of DEMP and CEES.

**J. Zhang *et al.* [108] (2012)** have studied the effects of Surface and morphological properties and impedance change on zeolite (NaY) and cerium oxide coating zeolite material towards DMMP (dimethyl methyl phosphonate). Comparative study of three zeolite sensors including pure NaY zeolite based, NaY coated with 30% $CeO_2$ and 3 μm films was used for detection of ~100 ppm DMMP at 320°C at fixed frequency of 3 kHz. On increasing the concentrations of $CeO_2$, impedance remained unchanged but response time was increased. It was found that membrane of zeolite based material show greater response in comparison to the pressed pellets of NaY and $CeO_2$-coated NaY. Finally it has reported that cerium oxide coating can successfully improve the recovery feature of the sensors, leading to desorption of DMMP.

**Y.C Hudiono *et al.* [109] (2012)** a new composite material was synthesized which act as highly breathable barrier material against mustard agent simulant (2-CEES). This composite material consists of two components: diol-RTIL polymer (a cross linked diol-functionalized room temperature ionic liquid polymer) and zeolite (NaY). The hydroxylated polymer component renders high water vapor penetrability whereas the basic zeolite renders reactive blocking of CEES vapor.

**Ji. Xinming *et al.* [110] (2011)** have reported adsorption-desorption behavior of Nanozeolites *i.e.* silicate-1, ZSM and Cu-ZSM-5 as adsorbent for DMMP (Dimethyl Methyl phosphonate). It has been found that Cu-ZSM-5 had highest adsorption capacity and best selectivity due to increase in proportion to copper content. The sensitivity and detection limit was observed with Cu-ZSM-5 about 8.8 Hz/ppm and 0.3 ppm, respectively, which confirm that zeolite Cu-ZSM-5 is good adsorbent for the detection of DMMP. The maximum adsorption capacity of Cu-ZSM was found when the copper content was more than 2.72%.

**B. Nazari *et al.* [111] (2010)** have been reported comparative study of MgO

particles synthesized in laboratory and technical grade. The method of synthesis was used very easier and effective. The ability of different types of MgO particles for the destruction of chemical warfare agents (CWA) simulants malathion (VX simulant) and DMMP (GB simulant). In this investigation it was found that the weight ratios of 1:16 and 1:32 (stimulant: MgO particles) decompose almost all of the CWA simulants. It was also found that the weight ratio of 1:32 could destroy the other destruction products. The characterization techniques UV-Vis and BET used for investigation. BET analysis showed that specific surface area (SSA) of the synthesized MgO particles and technical grade of MgO powders was found ~30.96 m$^2$/g and ~166.86 m$^2$/g respectively and synthesized MgO particles and technical grade of MgO powders had an average particle size of 75 nm and 20 micrometers, respectively. This study concludes that MgO particles showed a greater potential in the destruction of simulants of chemical warfare agents with a simple and low cost effective method.

L. Bromberg *et al.* [90] (2009) reported the compound PANOx and PHA were very reactive and obtained by one-step oximation of polyacrylonitrile and polyacrylamide, respectively. Synthesized compound polyacrylamidoxime (PANOx) and poly (N-hydroxyacrylamide) (PHA) shows nucleophilic hydrolysis towards chemical warfare agents (CWA) S-2-(diisopropylamino) ethyl O-ethyl methylphosphonothioate (VX), O-pinacolyl methylphosphonofluoridate (Soman, or GD), and isopropyl methylphosphonofluoridate (Sarin, or GB). The specific synthesized polymers (PANOx and PHA) were converted into their corresponding oximate salts which have greater pH values than the p$K$a *i.e.* 7.5 and 10.8 respectively. The synthesized PANOx and PHA showed spontaneous hydrolysis at moderate temperature and humidity. The conversion of the hydroxamate into the unreactive carboxylic groups was insignificant, so that the polymers maintained reactivity at mild conditions. The half-lives of VX in heterogeneous hydrolysis were measured in the presence of PANOx and PHA from 0.093 to 4.3 and 7.7 h, which obey pseudo-first order kinetics in the polymer dispersions. The rates of hydrolysis of PANOx towards VX exhibited a strong dependency on the degree of conversion of the amidoxime to amidoximate groups and in case of GB half-life was found less than 3 min. The nontoxic nature, greater catalytic efficiency and mode of synthesis for PANOx and PHA polymers make them attractive materials in decontamination. The degradation pathway is shown in Figure 20(a) and Figure 20(b). This study concludes the compounds PANOx and PHA are obtained by a simple oximation method with high yields and contain 3 - 10 mmol of reactive groups (amidoximate or hydroxamate) per gram of dry polymer.

In the presence of water, PANOx and PHA hydrolyzed GD and VX with great interest having half lives shorter than those in alkaline water. Due to simplicity in synthetic process, low cost of the precursor and greater degradation efficiency makes PANOx and PHA attractive in today's scenario.
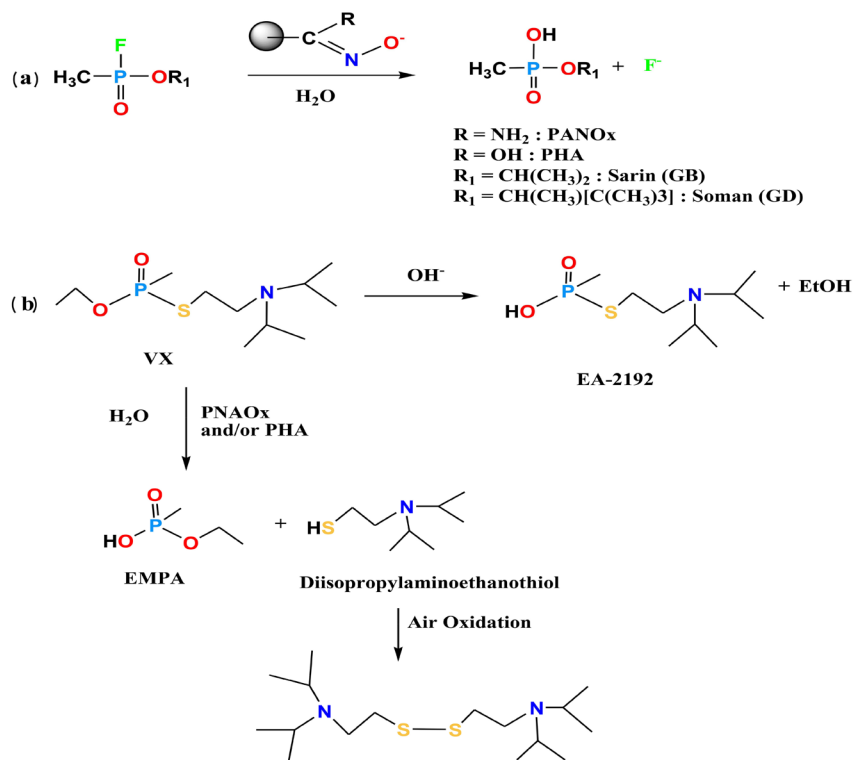
(a) $H_3C-\overset{F}{\underset{O}{P}}-OR_1$    $\overset{R}{\underset{N}{C}}=O^-$    $\xrightarrow{H_2O}$    $H_3C-\overset{OH}{\underset{O}{P}}-OR_1 \;+\; F^-$

R = NH$_2$ : PANOx
R = OH : PHA
R$_1$ = CH(CH$_3$)$_2$ : Sarin (GB)
R$_1$ = CH(CH$_3$)[C(CH$_3$)3] : Soman (GD)

(b) VX $\xrightarrow{OH^-}$ EA-2192 + EtOH

VX $\xrightarrow[\text{PNAOx and/or PHA}]{H_2O}$ EMPA + Diisopropylaminoethanothiol $\xrightarrow{\text{Air Oxidation}}$

**Figure 20.** (a) Degradation of GB and GD by PANOx and PHA in presence of water; (b) Degradation pathways of VX in the presence of alkali versus those in presence of PNAOx and PHA.

H. Grassian *et al.* [7] (2008) has reported the degradation of DMMP (dimethyl methyl phosphate, simulant of Sarin) nerve agents and 2-CEES (2-chloroethyl ethyl sulphate, simulant of sulfur mustard) blister agents by using three different nanocrystalline zeolites *i.e.* NaY, NaZSM-5 and silicalite. Nanocrystalline NaZSM-5 was found better degradent than the other two zeolites. It was found that CEES was decomposed by all the three zeolites (NaZSM-5, silicalite and NaY zeolite) whereas DMMP was degraded by only NaY zeolite. The adsorption was monitored by flow reactor apparatus and thermal conductivity detector (TCD) of GC. NaZSM-5 shows greater reactivity than silicalite. 20% more 2-CEES was adsorbed on its surface as compared to silicalite.

A. Kilincarslan *et al.* [112] (2007) reported synthesized PAN/zeolite composite has good adsorption capacity towards Th(IV) from aqueous solutions by using a batch technique. The parameters use for thorium adsorption was studied as pH, concentration, shaking time and temperature. The interpreted data fit into Langmuir, Freundlich and D-R type adsorption and desorption isotherms. In this study it was found with hydrochloride acid solution, desorption of Th(IV) is very slow and percent for this adsorbent was only found 14.48%. As a result of this, creating different chemical forms of Th(IV) with some components of the composite adsorbent and investigated the adsorption process. This study concludes that adsorbent is low cost and very effective sorbent for Th(IV) ions and the synthesized PAN/zeolite composite adsorbent exhibited excellent

adsorption for Th(IV).

K. Knagge *et al.* [113] (2006) have been reported the thermal degradation of nerve agent simulant dimethyl methylphosphonate (DMMP) by using Nanocrystalline NaY. 31P MAS NMR study reported the formation of two non toxic phosphorus species *i.e.* DMP and HMPA. After complete thermal decomposition of DMMP, the disappearance of all these products with the exception of some strongly adsorbed phosphate species was observed. Adsorption and thermal reaction of DMMP in Nanocrystalline NaY with a crystal size of ~30 nm. DMMP adsorbs molecularly in nanocrystalline NaY at 25˚C. The FTIR spectroscopy of Gas-phase products of the reaction of DMMP and oxygen in Nanocrystalline NaY at 200˚C was carried out and determined to be carbon dioxide (major product), formaldehyde, and dimethyl ether as products. The reactivity ratio per gram of zeolite sample was comparable to other recent studies of metal oxides like MgO, $Al_2O_3$ and $TiO_2$. The reaction mechanism is shown in Figure 21.

W. George *et al.* [114] (1999) investigate the reactions of synthesized zeolites NaY and AgY with CW Agent VX, HD and their simulants DEPPT (O,S-diethyl phenylphosphonothioate) and CEPS (2-chloroethyl phenyl sulfide) at room temperature. The reaction mechanisms are shown in Figure 22(a) and Figure 22(b). NMR techniques (solid-state magic angle spinning) were used to study the reaction.

VX molecules undergo hydrolysis with NaY and AgY zeolites and ultimately cleavage of the P-S to yield EMPA (ethyl methylphosphonate) which was slowly convert into ethyl 2-(diisopropylamino)ethyl methylphosphonate. Similar reaction was observed for DEPPT on AgY and silver salt of ethyl phenylphosphonate was observed but DEPPT does not show reaction with NaY. Hence AgY catalyzed hydrolysis reaction was more appropriate for both VX and DEPPT. In Case of HD and CEPS the reactivity of NaY was more as compare to AgY and formed Toxic CH-TG sulfonium ion and non toxic HEPS (2-hydroxyethyl phenyl sulfide) product respectively. In Case of VX hydrolysis of the P-O bond was not observed on either AgY or NaY and the desulfurized by-product yield was found 78%.

## 8. Conclusion

The bluff of terrorist attacks and environmental hazards has drawn attention of research scientists towards study of CWA and their simulants. The number of papers was comprised in this review related to decontamination study of CWA and simulants of CWA. Zeolite materials, metal oxides and composites of zeolites due to their readily availability, user-friendly and eco-friendly nature have been the subjects of such studies, and various zeolite materials have been investigated in this regard. Nano-technology could also open a new window for serial formulations with intensify advantages like high surface area, high ion exchange capacity and high surface to volume ratio towards CWA. Nanoscale zeolite are
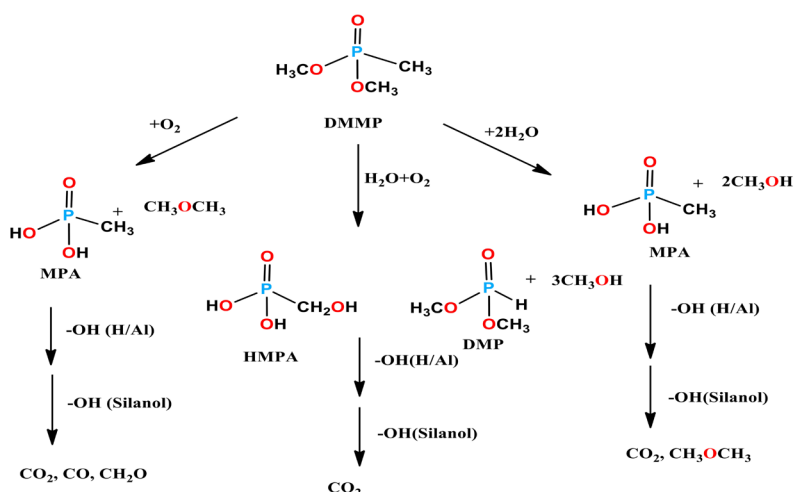
**Figure 21.** Thermal adsorption reaction of DMMP on the surface of zeolite NaY.
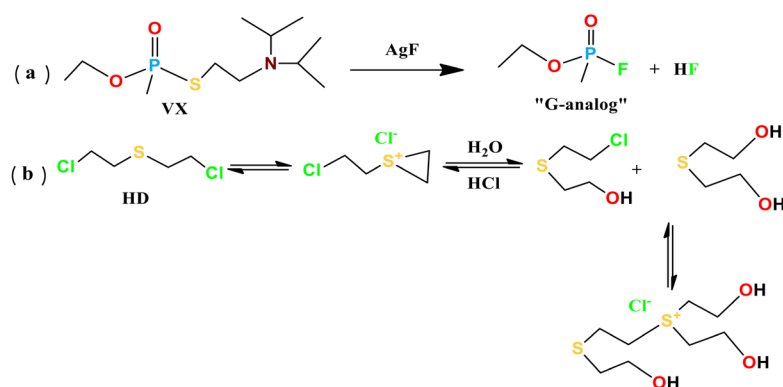


**Figure 22.** Reaction mechanism for (a) VX and (b) HD with metal halide nanoparticles.

more effective because of the presence of large surface area and pore volumes, low crystal defects, high ion exchange capacity etc. The products of degradation of CWA simulants on zeolite nanosurfaces have been examined experimentally. The correlation between the results for the real agents and their simulant implies that experiments performed with the simulant can be extrapolated to understand the mechanism for the real agents. Though large number of experimental results regarding the adsorption and degradation/decontamination of CWA on nanoscale zeolite and their simulants has accumulated over the years, this work has to be done to find materials for the early detection and degradation/decontamination of CWAs as well its simulants. In particular, large porous size and surface area zeolite and doped zeolite nanoparticles need to be explored further, as they have shown promise as future materials for CWA adsorption and degradation. Further research is necessary to determine the yet undetermined parameters like adsorption behaviour and mechanisms in zeolite-composite reactions.

## Conflicts of Interest

Conflict of interest on behalf of all co-authors, the corresponding author states

that this article content has no conflict of interest.

## Acknowledgements

## References

[1] Gangele, R., Pawaiya, P. and Pandey, Y. (2014) Synthetic Zeolites-Structure Properties and Application Area. *International Journal of Scientific Research*, **3**, 78.

[2] Breck, D.W. (1974) Zeolite Molecular Sieves: Structure, Chemistry and Use. John Wiley and Sons, London.

[3] Bekkum, V.H., Flanigen, E.M., Jacobs, P.A. and Jansen, J.C. (1991) Introduction to Zeolite Science and Practice. 2nd Edition, Elsevier, Amsterdam.

[4] Elshorbagy, W. and Chowdhury, R.K. (2013) Water Treatment. Chapter 5, InTech, London. https://doi.org/10.5772/2883

[5] https://www.crystalmarketreport.com/global-zeolite-for-detergents-market-research-report

[6] Georgiev, D., Bogdanov, B., Angelova, K., Markovska, I. and Hristov, Y. (2009) Synthetic Zeolites-Structure, Classification, Current Trends in Zeolite Synthesis. *International Science Conference*, Stara Zagora, 4-5 June 2009, 1-5.

[7] Grassian, V.H. and Larsen, S.C. (2008) Applications of Nanocrystalline Zeolites to CWA Decontamination. In: *Nanoscience and Nanotechnology for Chemical and Biological Defense*, Chapter 19, American Chemical Society, Washington DC, 249-260. https://doi.org/10.1021/bk-2009-1016.ch019

[8] Bhardwaj, D., Tomar, R., Khare, P.S., Goswami, Y. and Srivastva, P. (2013) Hydrothermal Synthesis and Characterization of Zeolite: Effect of Crystallization Temperature. *Research Journal of Chemical Sciences*, **3**, 1.

[9] Xu, R., Pang, W., Yu, J., Huo, Q. and Chen, J. (2007) Chemistry of Zeolites and Related Porous Mate Rials: Synthesis and Structure. John Wiley & Sons Ltd., Singapore.

[10] Smith, J.V. (1988) Topochemistry of Zeolites and Related Materials. 1. Topology and Geometry. *Chemical Reviews*, **88**, 149-182. https://doi.org/10.1021/cr00083a008

[11] Szostak, R. (1989) Molecular Sieves: Principles of Synthesis and Identification. 2nd Edition, Blackie Academic and Professional, London.

[12] Lutz, W. (2014) Zeolite Y: Synthesis, Modification, and Properties—A Case Revisited. *Advances in Materials Science and Engineering*, **2014**, Article ID: 724248. https://doi.org/10.1155/2014/724248

[13] Flanigan, E.M. (1980) Molecular Sieve Zeolite Technology: The First Twenty-Five Year. *Proceedings of the 5th International Conference on Zeolites*, Italy, 760-780.

[14] Moshoeshoe, M., Nadiye-Tabbiruka, M.S. and Obuseng, V. (2017) A Review of the Chemistry, Structure, Properties and Applications of Zeolites. *American Journal of Materials Science*, **7**, 196-221.

[15] Venuto, P.B. and Habib Jr., E.T. (1978) Catalyst-Feedstock-Engineering Interactions in Fluid Catalytic Cracking. *Catalysis Reviews: Science and Engineering*, **18**, 1-150. https://doi.org/10.1080/03602457808067529

[16] Rawlence, D.J. and Gosling, K. (1988) FCC Catalyst Performance Evaluation. *Ap-

*plied Catalysis*, **43**, 213-237. https://doi.org/10.1016/S0166-9834(00)82729-3

[17] Kerr, G.T. (1968) Chemistry of Crystalline Aluminosilicates. V. Preparation of Aluminum-Deficient Faujasites. *The Journal of Physical Chemistry*, **72**, 2594-2596. https://doi.org/10.1021/j100853a058

[18] Beyer, H.K., Belenykaja, I.M., Hange, F., Tielen, M., Grobet, P.J. and Jacobs, P.A. (1985) Preparation of High-Silica Faujasites by Treatment with Silicon Tetrachloride. *Journal of the Chemical Society*, *Faraday Transactions* 1: *Physical Chemistry in Condensed Phase*, **81**, 2889-2901. https://doi.org/10.1039/f19858102889

[19] Modhera, B., Chakraborty, M., Parikh, P.A. and Jasra, R.V. (2009) Synthesis of Nano-Crystalline Zeolite *β*: Effects of Crystallization Parameters. *Crystal Research and Technology*, **44**, 379-385. https://doi.org/10.1002/crat.200800474

[20] Kumar, P., Mal, N., Oumi, Y., Yamanaa, K. and Sanoc, T. (2001) Mesoporous Materials Prepared Using Coal Fly Ash as the Silicon and Aluminium Source. *Journal of Materials Chemistry*, **11**, 3285-3290. https://doi.org/10.1039/b104810b

[21] Zeng, R., Umana, J.C., Querol, X., Lopez, S.A., Plana, F. and Zuhang, X. (2002) Zeolite Synthesis from High Silicon Aluminium Fly Ash from East China. *Journal of Chemical Technology & Biotechnology*, **77**, 267-273. https://doi.org/10.1002/jctb.598

[22] Economics of Zeolite (1988) Reports on Metal and Minerals. Roskill Information Services Ltd.

[23] Hollman, G.G., Steenbruggen, G. and Janssen, J.M. (1999) A Two Step Process for Synthesis of Zeolite from Coal Fly Ash. *Fuel*, **78**, 1225-1230. https://doi.org/10.1016/S0016-2361(99)00030-7

[24] Park, M., Choi, C.L., Lim, W.T., Kim, M.C., Choi, J. and Heo, N.H. (2004) Molten-Salt Method for the Synthesis of Zeolite Materials I; Zeolite Formation in Alkaline Molten Salt System. *Microporous and Mesoporous Materials*, **27**, 555-564.

[25] Rayalu, S., Meshram, S.U. and Hasan, M.Z. (2002) Highly Crystalline Faujasitic from Fly Ash. *Journal of Hazardous Materials*, **77**, 123-131. https://doi.org/10.1016/S0304-3894(00)00212-0

[26] Inada, M., Eguchi, Y., Enomoto, N. and Hojo, J. (2005) Synthesis of Zeolite from Coal Fly Ashes with Different Silica Aluminium Composition. *Fuel*, **84**, 299-304. https://doi.org/10.1016/j.fuel.2004.08.012

[27] Querol, X., Moreno, N., Alastuey, A., Juan, R., Andrew, J.M., Lopez-Soler, A., Ayora, C., Medinaceli, A. and Valero, A. (2007) Synthesis of High Ion Exchange Zeolites from Coal Fly Ash. *Geologica Acta*, **5**, 49-57.

[28] Lolay, P.K. and Singh, D.N. (2001) Physical, Chemical Minerological and Thermal Properties of Canospheres from an Ash Lagoon. *Cement and Concrete Research*, **31**, 539-542. https://doi.org/10.1016/S0008-8846(01)00457-4

[29] http://www.lenntech.pl/zeolites-applications.htm

[30] Kulprathipanja, S. (2010) Zeolites in Industrial Separation and Catalysis. Wiley-VCH Verlag GmbH & Co. KGaA, Weinheim. https://doi.org/10.1002/9783527629565

[31] Murata, K.J., Firmoso, M.L.L. and Roisenberg, A. (1987) Distribution of Zeolites in Lavas of Southeastern Parana Basin, State of Rio Grande Do Sul, Brazil. *The Journal of Geology*, **95**, 455-467. https://doi.org/10.1086/629143

[32] Meng, X. and Xiao, F.S. (2014) Green Routes for Synthesis of Zeolites. *Chemical Reviews*, **114**, 1521-1543. https://doi.org/10.1021/cr4001513

[33] Wu, Q., Liu, X., Zhu, L., Ding, L., Gao, P., Wang, X., Pan, S., Bian, C., Meng, X., Xu, J., Deng, F., Maurer, S., Muller, U. and Xiao, F.S. (2015) Solvent-Free Synthesis of

Zeolites from Anhydrous Starting Raw Solids. *Journal of the American Chemical Society*, **137**, 1052-1055. https://doi.org/10.1021/ja5124013

[34] Meng, X., Wu, Q., Chen, F. and Xiao, F.S. (2015) Solvent-Free Synthesis of Zeolite Catalysts. *Science China Chemistry*, **58**, 6-13. https://doi.org/10.1007/s11426-014-5252-2

[35] Conner, W.C., Tompsett, G., Lee, K.H. and Sigfrid Yngvesson, K. (2004) Microwave Synthesis of Zeolites: 1. Reactor Engineering. *The Journal of Physical Chemistry*, **108**, 13913-13920. https://doi.org/10.1021/jp037358c

[36] Weller, M.T. and Dannl, S.E. (1998) Hydrothermal Synthesis of Zeolites. *Current Opinion in Solid State & Materials Science*, **3**, 137-l43. https://doi.org/10.1016/S1359-0286(98)80078-8

[37] Holmes, S.M., Alomair, A.A. and Kovo, A.S. (2012) The Direct Synthesis of Pure Zeolite—A Using 'Virgin' Kaolin. *RSC Advances*, **2**, 11491-11494. https://doi.org/10.1039/c2ra22263a

[38] http://www.personal.utulsa.edu/~geoffrey-price/zeolite/beta.htm

[39] Lee, T.P., Saada, B., Nga, E.P. and Salleh, B. (2012) Zeolite Linde Type L as Micro-Solid Phase Extraction Sorbent for the High Performance Liquid Chromatography Determination of Ochratoxin A in Coffee and Cereal. *Journal of Chromatography A*, **1237**, 46-54. https://doi.org/10.1016/j.chroma.2012.03.031

[40] de Sousa Jr., L.V., Silva, A.O.S., Silva, B.J.B. and Alencar, S.L. (2014) Synthesis of ZSM-22 in Static and Dynamic System Using Seeds. *Modern Research in Catalysis*, **3**, 49-56.

[41] Wadood Khan, A.L., Kotta, S., Husain Ansari, S., Ali, J. and Sharma, R.K. (2013) Recent Advances in Decontamination of Chemical Warfare Agents. *Defence Science Journal*, **63**, 487-496.

[42] Cheng, S., Wei, Y., Feng, Q., Qiu, K.Y., Pang, J.B., Jansen, S.A., Yin, R. and Ong, K. (2003) Facile Synthesis of Mesoporous Gold-Silica Nanocomposite Materials via Sol-Gel Process with Nonsurfactant Templates. *Chemistry of Materials*, **15**, 1560-566. https://doi.org/10.1021/cm0202106

[43] Haugen, D.M. (2001) Biological and Chemical Weapons. Green Haven Press, Inc., San Diego, CA.

[44] Lisa, M.E., Tobin, J.D. and Kim, D.J. (2007) Technological Advancements for the Detection of and Protection against Biological and Chemical WARFARE agents. *Chemical Society Reviews*, **36**, 458-470.

[45] Christopher, G.W., Cieslak, T.J., Pavlin, J.A. andEitzen Jr., E.M. (1997) Biological Warfare: A Historical Perspective. *The Journal of the American Medical Association*, **278**, 412-417.

[46] Geissler, E. (1986) Biological and Toxin Weapons Today. Oxford University Press Inc., New York.

[47] Wiener, S.W. and Hoffman, R.S. (2004) Nerve Agents: A Comprehensive Review. *Journal of Intensive Care Medicine*, **19**, 22-37. https://doi.org/10.1177/0885066603258659

[48] Worek, F., Wille, T., Koller, M. and Thiermann, H. (2016) Toxicollogy of Organophosphorus Compounds in View of an Increasing Terrorist Threat. *Archives of Toxicology*, **90**, 2131-2145. https://doi.org/10.1007/s00204-016-1772-1

[49] Vijayaraghavan, R., Kulkarni, A., Pant, S.C., Kumar, P., Rao, P.V.L., Gupta, N., Gautam, A. and Ganesan, K. (2005) Differential Toxicity of Sulfur Mustard Administered through Percutaneous, Subcutaneous, and Oral Routes. *Toxicology and*

*Applied Pharmacology*, **202**, 180-202. https://doi.org/10.1016/j.taap.2004.06.020

[50] https://www.sciencehistory.org/distillations/a-brief-history-of-chemical-war

[51] Rodriguez-Llanes, J.M., Guha-Sapir, D., Schlüter, B.-S. and Hsiao-Rei Hicks, M. (2018) Epidemiological Findings of Major Chemical Attacks in the Syrian War Are Consistent with Civilian Targeting: A Short Report. *Conflict and Health*, **12**, Article No. 16. https://doi.org/10.1186/s13031-018-0150-4

[52] Sharma, N. and Kakkar, R. (2013) Recent Advancements on Warfare Agents/Metal Oxides Surface Chemistry and Their Simulation Study. *Advanced Materials Letters*, **4**, 508-521.

[53] Ganesan, K., Raza, S.K. and Vijayaraghavan, R. (2010) Chemical Warfare Agents. *Journal of Pharmacy and Bioallied Sciences*, **2**, 166-178. https://doi.org/10.4103/0975-7406.68498

[54] Munro, N.B., Watson, A.P., Ambrose, K.R. and Griffin, G.D. (1990) Treating Exposure to Chemical Warfare Agents: Implications for Health Care Providers and Community Emergency Planning. *Environmental Health Perspectives*, **89**, 205-215. https://doi.org/10.1289/ehp.9089205

[55] Singh, B., Prasad. G.K., Pandey. K.S., Danikhel, R.K. and Vijayaraghavan, R. (2010) Decontamination of Chemical Warfare Agents. *Defence Science Journal*, **60**, 428-441.

[56] https://en.wikipedia.org/wiki/Blood_agent

[57] https://www.britannica.com/technology/chemical-weapon

[58] http://en.chembase.cn/substance-174275.html

[59] https://en.wikipedia.org/wiki/Phosgene

[60] https://en.wikipedia.org/wiki/Diphenylcyanoarsine/media/File:Clark-2.svg

[61] Beswick, F.W. (1983) Chemical Agents Used in Riot Control and Warfare. *Human & Experimental Toxicology*, **2**, 247-256. https://doi.org/10.1177/096032718300200213

[62] Allantyne, B. (1977) Riot Control Agents (Biomedical and Health Aspects of the Use of Chemicals in Civil Disturbances). In: Scott, R.B. and Frazer, J., Eds., *Medical Annual*, Wright and Sons, Bristol, 7.

[63] Bennett, S.R., *et al.* (1984) Environmental Hazards of Chemical Agent Simulants. CRDCTR-84055. US Army Armament, Munitions, and Chemical Command, Aberdeen Proving Ground, MD.

[64] Bartelt-Hunt Shannon, L., Knappe Detlef, R.U. and Barlaz Morton, A. (2008) A Review of Chemical War fare Agent Simulants for the Study of Environmental Behavior. *Critical Reviews in Environmental Science and Technology*, **38**, 112-136. https://doi.org/10.1080/10643380701643650

[65] Hiscock, J.R., Bustone, G.P. and Clark, E.R. (2017) Decontamination and Remediation of the Sulfur Mustard Simulant CEES with "Off-the-Shelf" Reagents in Solution and Gel States: A Proof-of-Concept Study. *Chemistry Open*, **6**, 497-500. https://doi.org/10.1002/open.201700063

[66] Ghabili, K., Agutter Paul, S., Ghanei, M., Ansarin, K., Panahi, Y. and Shoja Mohammadali, M. (2011) Sulfur Mustard Toxicity: History, Chemistry, Pharmacokinetics, and Pharmacodynamics. *Critical Reviews in Toxicology*, **41**, 384-403. https://doi.org/10.3109/10408444.2010.541224

[67] Smith Matthew, E. and Swoboda Henry, D. (2019) V-Series (Ve, Vg, Vm, Vx) Toxicity. StatPearls Publishing.

[68] https://en.wikipedia.org/wiki/Lewisite

[69] Pechura, C.M. and Rall, D.P. (1993) Committee on the Survey of the Health Effects of Mustard Gas and Lewisite. Institute of Medicine, National Academies Press, Washington DC.

[70] Gorzkowska-Sobas, A.A. (2013) Norwegian Defence Research Establishment (FFI), FFI-Rapport.

[71] Sferopoulos, R. (2008) A Review of Chemical Warfare Agent (CWA) Detector Technologies and Commercial-off-The-Shelf Items, Australian Government Department of Defense Research, DSTO-GD-0570.

[72] The Royal Society (2004) Report on Making the UK Safer: Detecting and Decontaminating Chemical and Biological Agents. Science Advice Section the Royal Society 6-9 Carlton House Terrace London SW1Y 5AG.

[73] Smith, B.M. (2008) Catalytic Methods for the Destruction of Chemical Warfare Agents under Ambient Conditions. *Chemical Society Reviews*, **37**, 470-478.
https://doi.org/10.1039/B705025A

[74] Okun, N.M., Tarr, J.C., Hilleshiem, D.A., Zhang, L., Hardcastle, K.I. and Hill, C.L. (2006) Highly Reactive Catalysts for Aerobic Thioether Oxidation: The Fe-Substituted Polyoxometalate/Hydrogen Dinitrate System. *Journal of Molecular Catalysis A*: *Chemical*, **246**, 11-17. https://doi.org/10.1016/j.molcata.2005.10.006

[75] Singh, B.K. and Walker, A. (2006) Microbial Degradation of Organophosphorus Compounds. *FEMS Microbiology Reviews*, **30**, 428-471.
https://doi.org/10.1111/j.1574-6976.2006.00018.x

[76] Russell, A.J., Erbeldinger, M., Defrank, J.J., Kaar, J. and Drevon, G. (2002) Catalytic Buffers Enable Positive-Response Inhibition-Based Sensing of Nerve Agents. *Biotechnology and Bioengineering*, **77**, 352-357. https://doi.org/10.1002/bit.10152

[77] Rojas, H.M. and Moss R.A. (2002) Phosphorolytic Reactivity of o-Iodosylcarboxylates and Related Nucleophiles. *Chemical Reviews*, **102**, 2497-2522.
https://doi.org/10.1021/cr9405462

[78] Wagner, G.W., Procell, L.R., O'Connor, R.J., Shekar, M., Carnes, C.L., Kapoor, P.N. and Klabunde, K.J. (1999) Reactions of VX, GB, GD, and HD with Nanosize MgO. *Journal of the American Chemical Society*, **103**, 3225-3228.
https://doi.org/10.1021/jp984689u

[79] Wagner, G.W., Bartram, P.W., Koper, O. and Klabunde, K.J. (1999) Reactions of VX, GD, and HD with Nanosize MgO. *The Journal of Physical Chemistry B*, **103**, 3225-3228. https://doi.org/10.1021/jp984689u

[80] Li, S.T. and Klabunde, K.J. (1985) Thermally Activated Magnesium Oxide Surface Chemistry. Adsorption and Decomposition of Phosphorus Compounds. *Langmuir*, **1**, 600-605. https://doi.org/10.1021/la00065a015

[81] Wagner, G.W., Koper, O., Lucas, E., Decker, S. and Klabunde, K.J. (2000) Reactions of VX, GD, and HD with Nanosize CaO: Autocatalytic Dehydrohalogenation of HD. *The Journal of Physical Chemistry B*, **104**, 5118-5123.
https://doi.org/10.1021/jp000101j

[82] Wagner, G.W., Procell, L.R., O'Connor, R.J., Shekar, M., Carnes, C.L., Kapoor, P.N. and Klabunde, K.J. (2001) Reactions of VX, GB, GD, and HD with Nanosize $Al_2O_3$. Formation of Aluminophosphonates. *Journal of the American Chemical Society*, **123**, 1636-1644. https://doi.org/10.1021/ja003518b

[83] Mahato, T.H., Prasad, G.K., Singh, B., Acharya, J., Srivastava, A.R. and Vijayaraghavan, R. (2009) Nanocrystalline Zinc Oxide for the Decontamination of Sarin. *Journal of Hazardous Materials*, **165**, 928-932.
https://doi.org/10.1016/j.jhazmat.2008.10.126

[84] Mitchel, M.B., Sheinker, V.N. and Mintz, E.A. (1997) Adsorption and Decomposition of Dimethyl Methylphosphonate on Metal Oxides. *The Journal of Physical Chemistry B*, **101**, 11192-11203. https://doi.org/10.1021/jp972724b

[85] Gordon, W.O., Tissue, B.M. and Morris, J.R. (2007) Adsorption and Decomposition of Dimethyl Methylphosphonate on $Y_2O_3$ Nanoparticles. *The Journal of Physical Chemistry C*, **111**, 3233-3240. https://doi.org/10.1021/jp0650376

[86] Prasad, G.K., Mahato, T.H., Singh, B., Ganesan, K., Pandey, P. and Sekhar, K. (2007) Detoxification Reactions of Sulphur Mustard on the Surface of Zinc Oxide Nanosized Rods. *Journal of Hazardous Materials*, **149**, 460-464. https://doi.org/10.1016/j.jhazmat.2007.04.010

[87] Kleinhammes, A., Wagner, G.W., Kulkarni, H., Qi, Y., Zhang, J., Qin, L.C. and Wu, Y. (2005) Decontamination of 2-Chloroethyl Ethylsulfide Using Titanate Nanoscrolls. *Chemical Physics Letters*, **411**, 81-85. https://doi.org/10.1016/j.cplett.2005.05.100

[88] Prasad, G.K., Mahato, T.H., Pandey, P., Singh, B., Suryanarayana, M.V.S., Saxena, A. and Sekhar, K. (2007) Reactive Sorbent Based on Manganese Oxide Nanotubes and Nanosheets for the Decontamination of 2-Chloro-Ethyl Ethyl Sulphide. *Microporous and Mesoporous Materials*, **106**, 256-261. https://doi.org/10.1016/j.micromeso.2007.03.004

[89] Mahato, T.H., Prasad, G.K., Singh, B., Batra, K. and Ganesan, K. (2010) Mesoporous Manganese Oxide Nanobelts for Decontamination of Sarin, Sulphur Mustard and Chloro Ethyl Ethyl Sulphide. *Microporous and Mesoporous Materials*, **132**, 15-21.

[90] Bromberg, L., Schreuder Gibson, H., Creasy, W.R., McGarvey, D.J., Fry, R.A. and Alan Hatton, T. (2009) Degradation of Chemical Warfare Agents by Reactive Polymers. *Industrial & Engineering Chemistry Research*, **48**, 1650-1659. https://doi.org/10.1021/ie801150y

[91] Sadeghi, M., Yekta, S. and Babanezhad, E. (2014) MnO 2-AgX Zeolite Nanocomposite as an Adsorbent Catalyst for the Decontamination against Sulfur Mustard Simulants. *Caspian Journal of Chemistry*, **3**, 57-75.

[92] Agarwal, S.R., Subramanian, S. and Seeram, R. (2012) Functionalized Cellulose: PET Polymer Fibers with Zeolites for Detoxification against Nerve Agents. *Journal of Inorganic Materials*, **27**, 332-336. https://doi.org/10.3724/SP.J.1077.2011.11558

[93] Carniato, F., Bisio, C., Evangelisti, C., Psaro, R., Dal Santo, V., Costenaro, D., Marcheseand, L. and Guidotti, M. (2018) Iron-Montmorillonite Clays as Active Sorbents for the Decontamination of Hazardous Chemical Warfare Agents. *Dalton Transactions*, **47**, 2939-2948. https://doi.org/10.1039/C7DT03859C

[94] Abdul Majid, S., Ahmad Mir, M. and Mohammad Mir, J. (2018) Nitrate and Phosphate Sorption Efficiency of Mordenite versus Zeolite-A at the Convergence of Experimental and Density Functionalized Evaluation. *Journal of the Chinese Advanced Materials Society*, **6**, 691-705.

[95] Liu, Y., Du, X., Wang, J., Yin, Y., Wang, B., Zhao, S., Li, N. and Li, C. (2018) High Efficient Detoxification of Mustard Gas Surrogate Based on Nanofibrous Fabric. *Journal of Hazardous Materials*, **347**, 25-30. https://doi.org/10.1016/j.jhazmat.2017.12.041

[96] Florent, M., Gianna koudakis, D.A. and Bandosz, T.J. (2017) Mustard Gas Surrogate Interactions with Modified Porous Carbon Fabrics: Effect of Oxidative Treatment. *Langmuir*, **33**, 11475-11483. https://doi.org/10.1021/acs.langmuir.7b02047

[97] Li, J.X., Jiang, B.Q., Liu, Y., Qiu, C.Q., Hu, J.J., Qian, G.R., Guo, W.S. and Ngo, H.H.

(2017) Preparation and Adsorption Properties of Magnetic Chitosan Composite Adsorbent for Cu$^{2+}$ Removal. *Journal of Cleaner Production*, **158**, 51-58. https://doi.org/10.1016/j.jclepro.2017.04.156

[98] Sadeghi, M., Yekta, S. and Ghaedi, H. (2016) Decontamination of Chemical Warfare Sulfur Mustard Agent Simulant by ZnO Nanoparticles. *International Nano Letters*, **6**, 161-171. https://doi.org/10.1007/s40089-016-0183-x

[99] Vaclav Stengl, M.S., Henych, J., Tolasz, J., Vomacka, P. and Ederer, J. (2016) Mesoporous Manganese Oxide for the Degradation of Organophosphates Pesticides. *Journal of Materials Science*, **51**, 2634-2642. https://doi.org/10.1007/s10853-015-9577-9

[100] Sadeghi, M., Ghaedi, H., Yekta, S. and Babanezhad, E. (2016) Decontamination of Toxic Chemical Warfare Sulfur Mustard and Nerve Agent Simulants by NiO NPs/Ag-Clinoptilolite Zeolite Composite Adsorbent. *Journal of Environmental Chemical Engineering*, **4**, 2990-3000. https://doi.org/10.1016/j.jece.2016.06.008

[101] Aono, H., Kaji, N., Itagaki, Y., Johan, E. and Matsue, N. (2016) Synthesis of Mordenite and Its Composite Material Using Chemical Reagents for Cs Decontamination. *Journal of the Ceramic Society of Japan*, **124**, 617-623.

[102] Dastafkan, K., Sadeghi, M. and Obeydavi, A. (2015) Manganese Dioxide Nanoparticles-Silver-Y Zeolite as a Nanocomposite Catalyst for the Decontamination Reactions of O, S-Diethyl Methyl Phosphonothiolate. *International Journal of Environmental Science and Technology*, **12**, 905-918. https://doi.org/10.1007/s13762-014-0701-1

[103] Singh, V.V., Jurado-Sánchez, B., Sattayasamitsathit, S., Orozco, J., Li, J., Galarnyk, M., Fedorak, Y. and Wang, J. (2015) Multifunctional Silver-Exchanged Zeolite Micromotors for Catalytic Detoxification of Chemical and Biological Threats. *Advanced Functional Materials*, **25**, 2147-2155.

[104] Kumar, J.P., Ramacharyulu, P.V.R.K., Prasad, G.K., Srivastava, A.R. and Singh, B. (2015) Molecular Sieves Supported with Metal Oxide Nanoparticles: Synthesis, Characterization and Decontamination of Sulfur Mustard. *Journal of Porous Materials*, **22**, 91-100. https://doi.org/10.1007/s10934-014-9876-6

[105] Khanday, W.A., Abdul Majid, S., Chandra Shekar, S. and Tomar, R. (2014) Dynamic Adsorption of DMMP over Synthetic Zeolite-Alpha. *Arabian Journal of Chemistry*, **7**, 115-123. https://doi.org/10.1016/j.arabjc.2013.06.026

[106] Khanday, W.A., Abdul Majid, S., Chandra Shekar, S. and Tomar, R. (2013) Synthesis and Characterization of Various Zeolites and Study of Dynamic Adsorption of Dimethyl Methyl Phosphate over Them. *Materials Research Bulletin*, **48**, 4679-4686. https://doi.org/10.1016/j.materresbull.2013.08.003

[107] Sharifi Alhashem, S.L. and Sadeghi, M. (2012) Preparation of Manganese Dioxide Nanoparticles/Zeolite AgY Composite and Investigation of its Reaction with 2-Chloro Ethyl Phenyl Sulfide and Dimethyl Methylphosphonate. *Passive Defence Science and Technology*, **2**, 169-178.

[108] Zhang, J., Li, X., White, J. and Dutta, P.K. (2012) Effects of Surface and Morphological Properties of Zeolite on Impedance Spectroscopy-Based Sensing Performance. *Sensors*, **12**, 13284. https://doi.org/10.3390/s121013284

[109] Hudiono, Y.C., Miller, A.L., Gibson, P.W., Lafarge, A.L., Noble, R.D. and Gin, D.L. (2012) A Highly Breathable Organic/Inorganic Barrier Material that Blocks the Passage of Mustard Agent Simulants. *Industrial & Engineering Chemistry Research*, **51**, 7453-7456. https://doi.org/10.1021/ie202977e

[110] Ji, X., Yao, W., Hu, Y., Ren, N., Zhou, J., Huang, Y. and Tang, Y. (2011) Adsorption

and Desorption Characteristics of Nanozeolites as Adsorbent for Dimethyl Methylphosphonate. *Sensors and Materials*, **23**, 303.

[111] Nazari, B. and Jaafari, M. (2010) A New Method for the Synthesis of MgO Nanoparticles for the Destructive Adsorption of Organo-Phosphorus Compounds. *Digest Journal of Nanomaterials and Biostructures*, **5**, 909-917.

[112] Kaygun, A.K. and Akyil, S. (2007) Study of the Behaviour of Thorium Adsorption on PAN/Zeolite Composite Adsorbent. *Journal of Hazardous Materials*, **147**, 357-362.
https://doi.org/10.1016/j.jhazmat.2007.01.020

[113] Knagge, K., Johnson, M., Grassian, V.H. and Larsen, S.C. (2006) Adsorption and Thermal Reaction of DMMP in Nanocrystalline NaY. *Langmuir*, **22**, 11077-11084.
https://doi.org/10.1021/la061341e

[114] Wagner, G.W. and Bartram, P.W. (1999) Reactions of VX, HD, and Their Simulants with NaY and AgY Zeolites. Desulfurization of VX on AgY. *Langmuir*, **15**, 8113-8118. https://doi.org/10.1021/la990716b